Chapter 4

# THERMOLUMINESCENCE MEASUREMENTS OF GAMMA RAYS

**Takashi Maruyama and Yoshikazu Kumamoto**
*National Institute of Radiological Sciences*

**Yoneta Ichikawa and Tsuneto Nagatomo**
*Nara University of Education*

**Masaharu Hoshi**
*Hiroshima University*

**Edwin Haskell and Prasad Kaipa**
*University of Utah*

Computation of radiation doses to survivors at Hiroshima and Nagasaki requires knowledge of factors including height and location of burst, neutron attenuation by the bomb casing, reflection of the blast wave by hills and buildings, and composition and orientation of objects in the vicinity of the survivors. Aspects of the computer models are tested on data from early nuclear tests and on results of open air reactor experiments designed to simulate critical parameters. Nonetheless the computation from detonation to dose to man is a formidable problem, and it is fortunate that both techniques and materials exist that can provide a direct comparison of theory to measured dose in materials which were present and exposed at the time of the bombings (Figure 1). The materials described in this chapter are ceramic bricks and tiles to which a thermoluminescence (TL) dosimetry technique was applied.

The present work follows by two decades the first TL studies performed on bricks and tiles at Hiroshima and Nagasaki.[1,2] In light of our present knowledge of the TL of natural minerals, the earlier studies may seem crude. The list of checks and counter checks developed for TL analysis since that time is large. Nevertheless, the values obtained in the earlier studies compare favorably with those obtained at a number of laboratories using modern techniques and instrumentation. Given the empirical basis of this study and the ease with

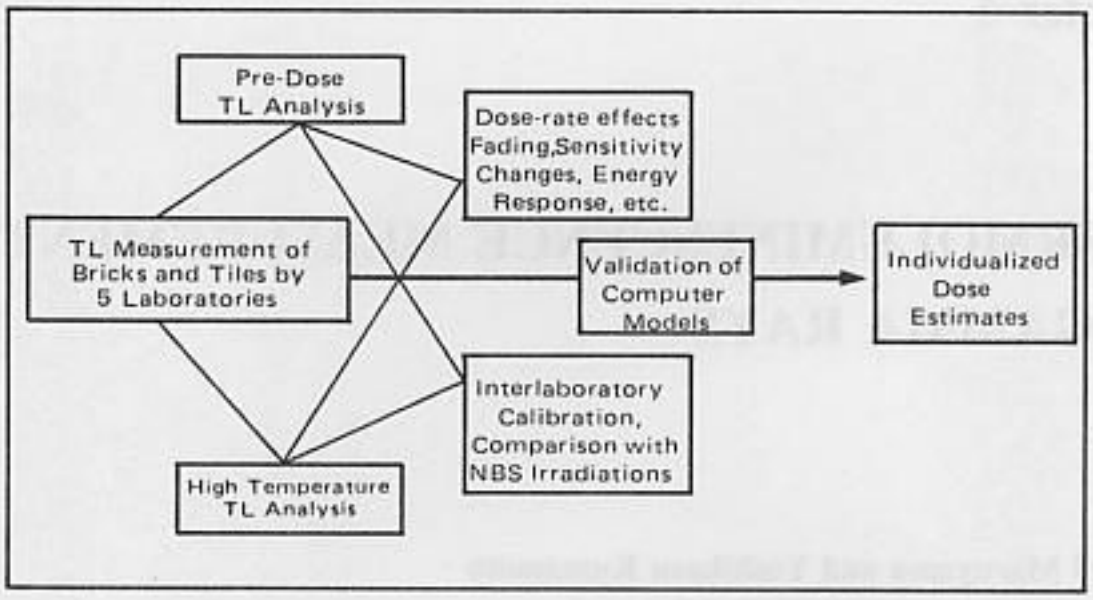


*Figure 1. Relationship of thermoluminescence effort to the dose reassessment project.*

which systematic errors may arise and remain undiscovered, the collaborative nature of this project has been fortunate. Laboratories participating directly in the measurements include the National Institute of Radiological Sciences (JNIRS in Chiba), and Nara University of Education (NUE in Nara) in Japan, the University of Utah (UU in Salt Lake City, Utah) in the United States, and Oxford and Durham Universities (OXF and DUR) in England.

**Historical Comments**

The first scientific report on TL was made by Robert Boyle to the Royal Society in 1663. His observation of visible light emitted from a diamond under the influence of mild heating was the precursor of modern TL dosimetry. The relationship of radiation to TL was established in the 19th century, but it was not until the availability of photomultiplier tubes and sensitive amplifiers that the potential of TL as a dosimetry technique was exploited, largely through the work of Farrington Daniels and his research group at the University of Wisconsin. Ironically, one of the first applications of TL to radiation dosimetry involved dosimetry of an A-bomb detonation in 1953 using LiF crystals,[3] while the first major application of the technique to dosimetry of contemporary environmental materials again involved A-bomb dosimetry.[1,2] The vast majority of the TL work has involved the development and characterization of highly sensitive phosphors suitable for radiation monitoring of individuals. TL dosimeters using LiF, BeO, $CaSO_4$, and $Li_2B_4O_7$ have almost entirely replaced film badges for personnel dosimetry.

TL also entered the field of archaeological dating with the application of the technique to ceramics in 1960.[4,5] The resulting association with ancient pottery has provided us with much of the scientific foundation for the present study. Other applications that have evolved for TL include techniques for geological prospecting, dating of ocean sediments, examination of meteorites and lunar samples, and techniques for defect analysis in solid state physics (Figure 2).

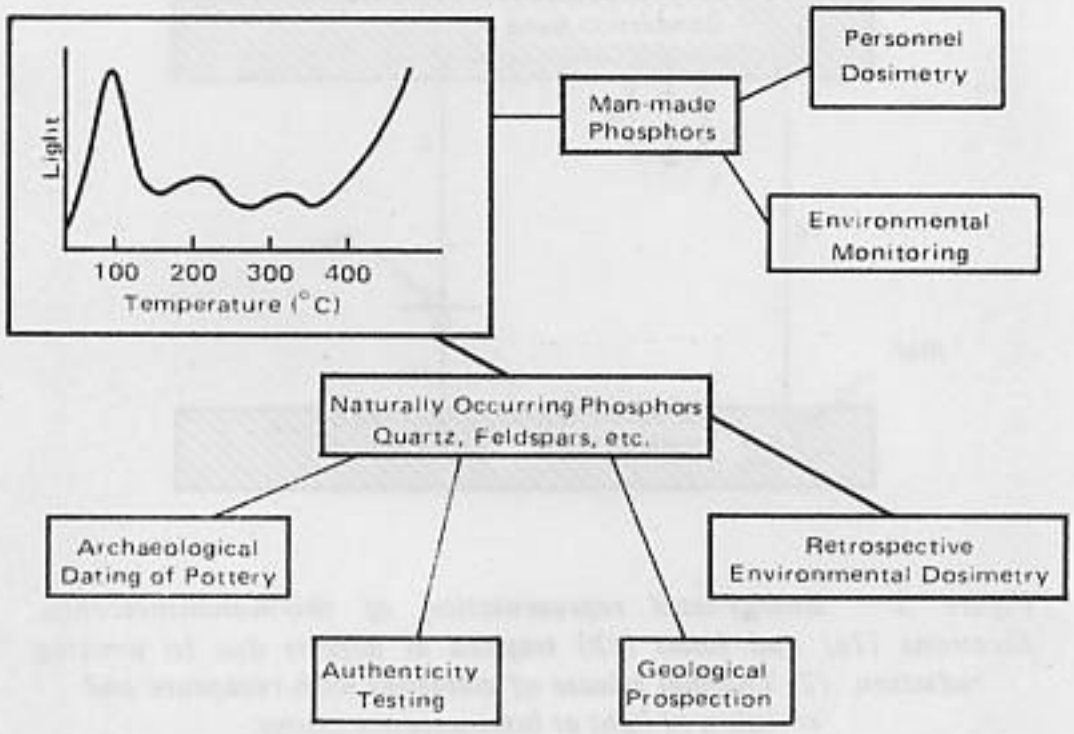


*Figure 2. Applications of thermoluminescence.*

## GENERAL ASPECTS OF THERMOLUMINESCENCE

Thermoluminescence may be defined as the thermally stimulated release of light from materials previously exposed to ionizing radiation. This definition distinguishes TL from other luminescence processes that occur during the application of the primary exciting agent such as pressure (piezoluminescence), friction (triboluminescence), light (photoluminescence), or chemical energy (chemiluminescence). It also distinguishes TL from the incandescent glow of the sample as it is heated to high temperatures. The TL process is "destructive" in that the signal is depleted and the phosphor "reset" as a dosimeter with each heating. Figure 2 shows TL output versus temperature (glow curve) for a quartz sample. Note the rise in the signal at higher temperatures due to incandescence.

A portion of the energy absorbed by a crystal during irradiation remains stored over time as electrostatic energy within the crystal lattice. This occurs due to the presence of impurities or lattice defects that act as traps for electrons or holes released during ionization. The band gap diagram of Figure 3 offers a simplified depiction of processes leading to TL in a solid with a single electron trap and a single hole trap, the latter also being a luminescence "center".

In the model the conduction band is separated from the valence band by the energy required for ionization (8.5 eV for quartz). Most of the electrons ejected into the conduction band by ionization quickly fall back to their original low-energy states in the valence band; however, a certain number are captured at electron traps "T" created by impurities or by vacancies in the band gap region. These trapped electrons are the "stored" TL signal. The lifetime of the electrons in the traps, and thus the stability of the stored signal over time, is

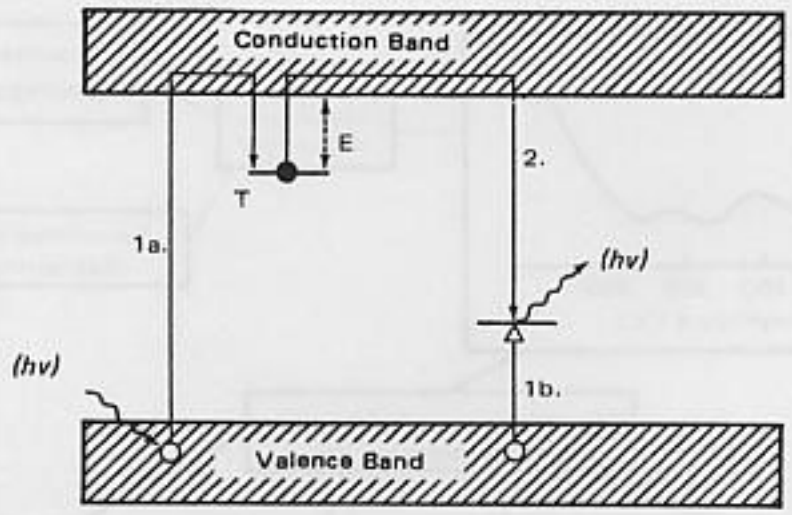


*Figure 3. Energy-level representation of thermoluminescence. Electrons (1a) and holes (1b) trapped at defects due to ionizing radiation. (2) Thermal release of electrons with recapture and emission of light at luminescence center.*

related to the trapping energy (or "trap depth") and to the temperature of the crystal by the equation:

$$t = \frac{exp(E/kT)}{s} \qquad (1)$$

where E is the distance between the trap and the conduction band, s is a constant, k is Boltzman's constant, and T is the absolute temperature.

When a sample is heated during TL readout, electrons are ejected from their traps at temperatures characteristic of the trap depth, and those captured in the band gap region by luminescence centers "L" emit light. The resulting plot of light output versus sample temperature (Figure 2) is termed a "glow curve". The portion of the glow curve in the lower temperature region results from electrons with shallow trap depths that can slowly be expelled from their traps even at normal temperatures. This portion will decrease or "fade" more rapidly with time than the high temperature portion of the glow curve.

Real materials must generally be described by multitrap models which are complicated by retrapping of electrons by either the original traps or competing traps following thermal ejection. The probability of trapping, retrapping, or luminescence is then a function of dose, resulting in nonlinearity of TL output and shifts in peak temperature with increasing dose. The current state of our knowledge of the traps and centers responsible for TL was summarized recently by McKeever.[6,7]

**Conventional Applications**

Conventional applications of TL dosimetry involve monitoring of individuals involved in radiation-related occupations, monitoring of areas which may be subject to radiation exposure, monitoring of normal environmental background levels, and measuring doses related

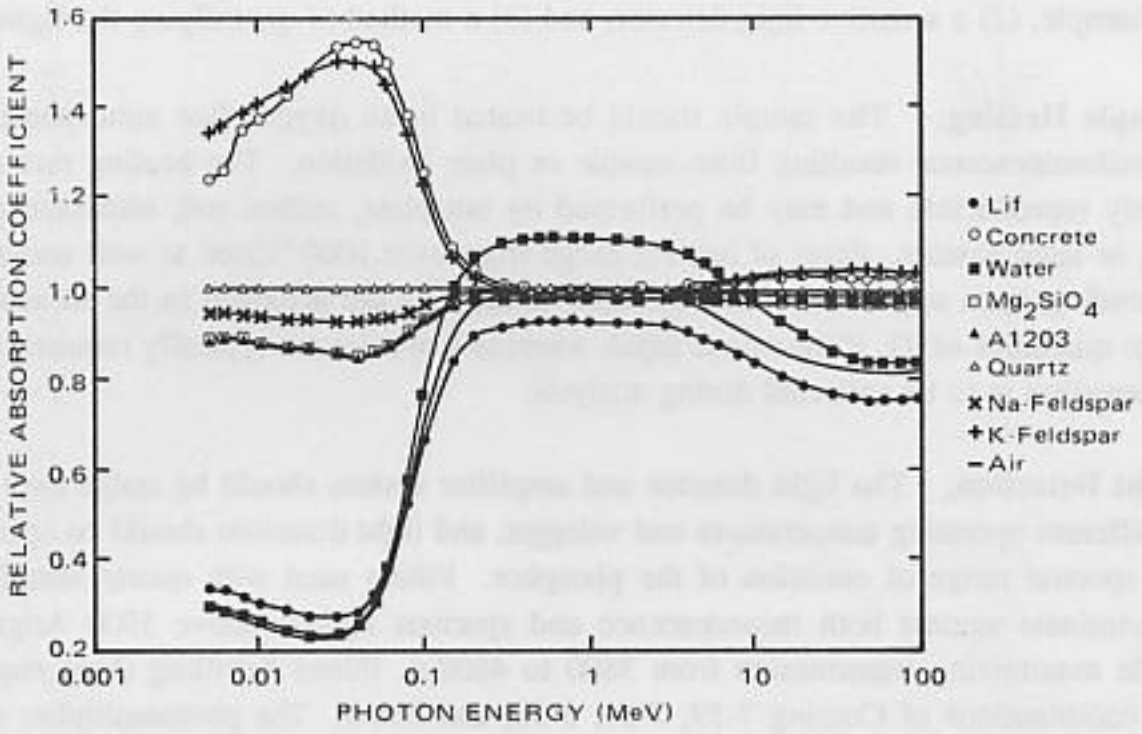


*Figure 4. Variation of energy absorption coefficient $(\mu/\rho)_{tot,en}$ relative to the energy absorption coefficient for quartz, for some relevant shielding materials, and for two "quartz equivalent" dosimeters.*

to therapeutic applications of radiation.

One of the most popular TL phosphors for personnel dosimetry, LiF (TLD 100, Harshaw Chemical Co.) was also the first developed on a commercial basis. It is favored because of its sensitivity, low fading, and roughly tissue-equivalent energy response to photons. That is, the dose of radiation indicated by the dosimeter differs negligibly from that absorbed by tissue when they are exposed in similar photon fields, regardless of the energy of the photons. As illustrated in Figure 4 quartz and other materials relevant to the present study are not tissue equivalent, particularly at low photon energies where the absorption coefficent, and thus the absorbed dose, increases as the cube of the atomic number of the absorber. The result for dosimetry purposes may be a severe overestimate of exposure if the low-energy component of the radiation is under estimated.

Other requirements for TL phosphors include: (1) stability of the signal over time (fading must be minimal, predictable, or monitored), (2) reproducibility of measurements must be such that errors associated with measurements of multiple aliquots of an irradiated sample are minimal, (3) TL must be insensitive to environmental factors such as humidity, light, moisture and temperature, (4) self irradiation from radionuclides in the phosphors themselves should be low, and (5) absorbed dose versus photon energy should correspond to that of tissue or other material for which dosimetry is undertaken. In addition, appropriate material should surround the phosphor to insure the buildup of secondary electrons.

**Instrumentation**

The basic instrumentation required for TL analysis includes: (1) a heating element for

the sample, (2) a sensitive light detector, and (3) a method of quantifying the light detected.

**Sample Heating.** The sample should be heated in an oxygen-free atmosphere to avoid chemiluminescence resulting from sample or plate oxidation. The heating rate should be highly reproducible and may be performed by hot plate, carbon rod, nichrome strips, hot gas, or laser heating. Rates of heating range from over 1000 °C/sec to well under 1 °C/sec depending upon application. Clearly, time advantages are achieved in the measurement of large quantities of TL if the rate is rapid, whereas low rates are typically required if spectral information is to be collected during analysis.

**Light Detection.** The light detector and amplifier system should be stable over time and at different operating temperatures and voltages, and light detection should be optimized for the spectral range of emission of the phosphor. Filters used with quartz samples should discriminate against both incandescence and spurious signals above 5500 Angstrom (A) while maximizing transmission from 3800 to 4800 A. Filters fulfilling these requirements are combinations of Corning 7-59, 7-51, 5-58, and HA-3. The photomultiplier tube must also be sensitive in this region (bialkali windows with transmission in the ultraviolet are typically preferred).

**Data Collection and Recording.** Data collection and recording devices range from the charging of a capacitor by the amplification of the photocathode output current to the storage of individual photon counts versus temperature. Output can be numeric (providing values for peak height or area), graphic (providing plots of glow curves), or a combination of the two. Computerized systems may provide additional capabilities by taking into account data collected from previous heatings or samples. A primary requirement of data output for research purposes is that quantitative information be available concerning the shape and size of individual glow curves.

## APPLICATION OF THERMOLUMINESCENCE TO A-BOMB DOSIMETRY

### Relationship to Archaeological Dating

Many of the requirements for TL phosphors listed above apply equally to commercial phosphors, to archaeological specimens, and to quartz extracted from tile or bricks in Hiroshima and Nagasaki. Fading and sensitivity to environmental parameters are especially relevant for A-bomb dosimetry since samples will have been in the field in excess of 40 years. Secondary electron buildup must be considered, as must energy response of both the crystal and surrounding matrix. Self dosing and dose contribution from other natural sources of radiation become increasingly important for older samples and for samples with low doses (less than 100 rad). In the dating of archaeological samples age is computed as follows:

$$A = \frac{TL}{\beta + \gamma + \alpha + c} \tag{2}$$

where

A = Age of sample since firing

| | | |
|---|---|---|
| TL | = | Dose measured with TL techniques |
| $\beta$ | = | $\beta$-particle component of natural dose-rate |
| $\gamma$ | = | $\gamma$-ray component of natural dose-rate |
| $\alpha$ | = | $\alpha$-particle component of natural dose-rate* |
| c | = | cosmic-ray component of natural dose-rate. |

The situation is even more demanding in the present case since the dose "TL" includes an additional dose due to A-bomb radiation "D". D is indistinguishable from the dose due to natural background, and to separate the two, the age of the sample must be known:

$$D = TL - A(\beta + \gamma + \alpha + c) \tag{3}$$

The error associated with the calculation is a function of the sample age as well as of the accuracy of the measurements.

$$\sigma_D = \sqrt{\sigma_{TL}^2 + \sigma_A^2[\beta + \gamma + \alpha + c]^2 + A^2[\sigma_\beta^2 + \sigma_\gamma^2 + \sigma_\alpha^2 + \sigma_c^2]} \tag{4}$$

where the standard errors are as follows:

| | | |
|---|---|---|
| $\sigma_D$ | = | Standard error of the A-bomb dose estimate |
| $\sigma_{TL}$ | = | Standard error of the TL dose measurement |
| $\sigma_A$ | = | Standard error of age estimate |
| $\sigma_\beta$ | = | Standard error of $\beta$ dose-rate measurement |
| $\sigma_\gamma$ | = | Standard error of $\gamma$ dose-rate measurement |
| $\sigma_\alpha$ | = | Standard error of $\alpha$ dose-rate measurement |
| $\sigma_c$ | = | Standard error of cosmic-ray dose-rate measurement. |

The effect of varying individual parameters on overall error was discussed at the 2nd Joint Workshop in 1983.[8]

Additional requirements for A-bomb dosimetry include knowledge of distance from the hypocenter, orientation of the sample, irradiation and heating history, degree of shielding, density, and, to a lesser extent, elemental composition. Given the difference in the energy response of quartz relative to that of tissue at low photon energies, a knowledge of the energy spectrum of the incident radiation is also required. The techniques used for measuring background dose, for preparation of samples, and for TL measurements themselves are derived largely from archaeological TL dating practices and are detailed below. Excellent reviews are provided in the following books.[7,9–11]

**Samples**

During the past four decades, Hiroshima and Nagasaki have undergone phenomenal reconstruction and few buildings remain as they were at the time of the bombings. Fortunately for our present purpose, several buildings remain essentially unchanged in Hiroshima at dis-

*Factors relating to the effectiveness of alpha particles in inducing TL must also be included.

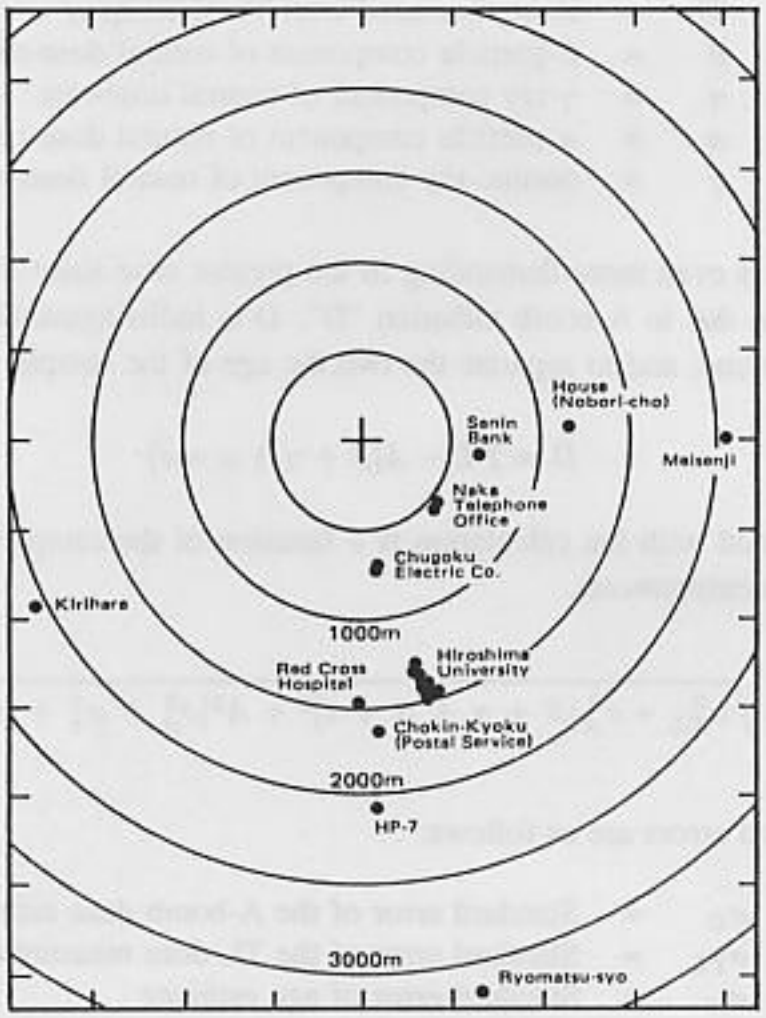


*Figure 5. Location of thermoluminescence samples in Hiroshima.*

tances of epidemiological interest, approximately 1400 m from the hypocenter. In Nagasaki, fewer structures are available and the most useful samples were bricks from the fence of a private house in Ieno-cho in Nagasaki, again at a distance of approximately 1400 m from the hypocenter. During the present dose reassessment, two original buildings in Hiroshima at 500 and 700 m from the hypocenter were demolished and a number of samples were collected from these buildings. In Nagasaki, small pieces of brick were collected mostly from fences of cemeteries. Sample coordinates are listed in Table 1, and the locations are shown in Figure 5 and 6. A detail of the main building sampled in Hiroshima, the Faculty of Sciences Building at Hiroshima University, is shown in Figure 7. Further details of the sampling sites are given in Appendix 4-11 and other appendixes to Chapter 4. In the collection of samples, it was important that:

1. The age of the building was known or could be closely approximated.
2. The samples had not been annealed by fires.
3. Artificial sources of radiation had not been present.
4. The samples were still attached to the structure.
5. Large scale remodeling had not occurred, or could be accurately documented.
6. The geometry, incident angle of radiation, and location and composition of nearby

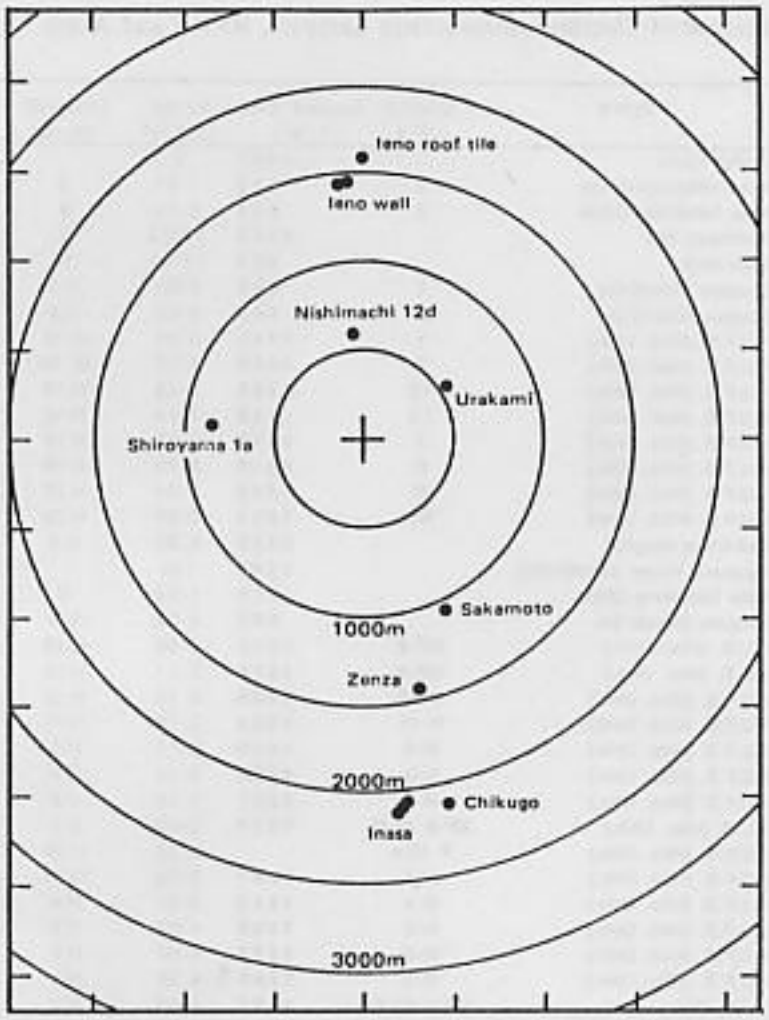


*Figure 6. Location of thermoluminescence samples in Nagasaki.*

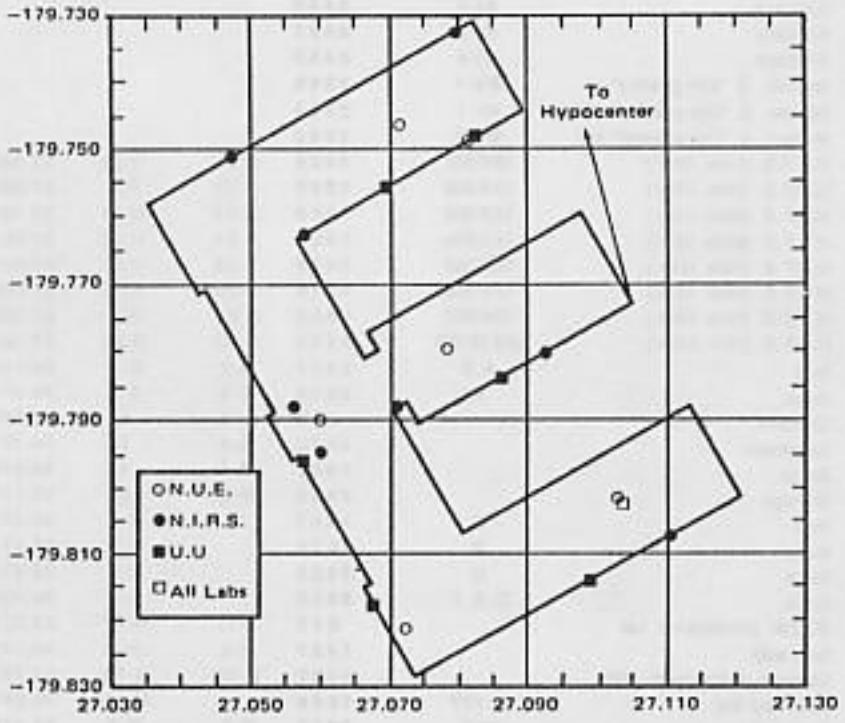


*Figure 7. Faculty of Science building at Hiroshima University. Location of thermoluminescence samples relative to New Map (RERF)*

## Table 1. Location of Thermoluminescence Samples, RERF and Army Map Comparison

| CITY | LABORATORY | PLACE | SAMPLE I.D. # | Quoted Dist *(m) | R.E.R.F. LIST NO. | NEW MAP FIG. NO. | NEW MAP COORDINATE | |
|---|---|---|---|---|---|---|---|---|
| H | J.N.I.R.S. | Chokin Kyoku | | 1607 | 2 | | | |
| H | J.N.I.R.S. | Naka Telephone Office | 3 | 515 | 1-01 | 2 | 27.128229 | -178.719284 |
| H | J.N.I.R.S. | Naka Telephone Office | 2 | 539 | 1-19 | 8 | 27.123345 | -178.749907 |
| H | J.N.I.R.S. | Ryomatsu-sho | | 3387 | 11-04 | 1 | 27.375499 | -181.466024 |
| H | J.N.I.R.S. | Sanin Bank | | 621 | 12-02 | 3 | 27.353532 | -178.454932 |
| H | J.N.I.R.S. | Chugoku Electric Co | 1 | 660 | 2-01 | H.1 | 26.800624 | -179.061621 |
| H | J.N.I.R.S. | Chugoku Electric Co | 2 | 680 | 2-03 | H.3 | 26.792291 | -179.088918 |
| H | J.N.I.R.S. | H.U.F.S. (Hiro. Univ.) | 1 | 1443 | 3-01 | H.19 | 27.110316 | -179.807179 |
| H | J.N.I.R.S. | H.U.F.S. (Hiro. Univ.) | 7 | 1366 | 3-07 | H. 14 | 27.080351 | -179.732443 |
| H | J.N.I.R.S. | H.U.F.S. (Hiro. Univ.) | 10 | 1368 | 3-10 | H.13 | 27.047544 | -179.751211 |
| H | J.N.I.R.S. | H.U.F.S. (Hiro. Univ.) | 14 | 1428 | 3-14 | H.10 | 27.070761 | -179.787869 |
| H | J.N.I.R.S. | H.U.F.S. (Hiro. Univ.) | I | 1393 | 3-28 | H.15 | 27.057822 | -179.762531 |
| H | J.N.I.R.S. | H.U.F.S. (Hiro. Univ.) | II | 1416 | 3-29 | H.16 | 27.056130 | -179.787768 |
| H | J.N.I.R.S. | H.U.F.S. (Hiro. Univ.) | IV | 1420 | 3-31 | H.25 | 27.092490 | -179.780047 |
| H | J.N.I.R.S. | H.U.F.S. (Hiro. Univ.) | R1 | 1433 | 3-35 | H.29 | | |
| H | J.N.I.R.S. | Red Cross Hospital | | 1433 | 5-01 | H.1 | 26.704789 | -179.850980 |
| H | N.U.E. | Japanese House (Naborl-cho) | | 1140 | 145 | - | 27.861500 | -178.297000 |
| H | N.U.E. | Naka Telephone Office | | 515 | 1-04 | C | 27.116973 | -178.757355 |
| H | N.U.E. | Chugoku Electric Co. | | 680 | 2-03 | H.3 | 26.792291 | -179.088918 |
| H | N.U.E. | H.U.S. (Hiro. Univ.) | HP-2 | 1359 | 3-08 | H.22 | 27.075490 | -179.735224 |
| H | N.U.E. | H.U.S. (Hiro. Univ.) | HP-3 | 1376 | 3-11 | H.23 | 27.044242 | -179.753100 |
| H | N.U.E. | H.U.F.S. (Hiro. Univ.) | H-10 | 1449 | 3-15 | H.10 | 27.103640 | -179.802397 |
| H | N.U.E. | H.U.F.S. (Hiro. Univ.) | H-11 | 1460 | 3-16 | H.11 | 27.072454 | -179.820935 |
| H | N.U.E. | H.U.F.S. (Hiro. Univ.) | H-9 | 1426 | 3-17 | H.9 | 27.060192 | -179.789914 |
| H | N.U.E. | H.U.F.S. (Hiro. Univ.) | H-8 | 1421 | 3-18 | H.8 | 27.078715 | -179.779318 |
| H | N.U.E. | H.U.F.S. (Hiro. Univ.) | H-6 | 1387 | 3-20 | H.6 | 27.071856 | -179.745909 |
| H | N.U.E. | H.U.S. (Hiro. Univ.) | HP-4 (H-6) | 1377 | 3-20 | H.6 | 27.071856 | -179.745909 |
| H | N.U.E. | H.U.F.S. (Hiro. Univ.) | ? 10.4 | | 3-35 | H.29 | 27.102843 | -179.801165 |
| H | N.U.E. | H.U.F.S. (Hiro. Univ.) | H-7 | 1397 | 3-36 | H.33 | 27.082036 | -179.748680 |
| H | N.U.E. | H.U.P.S. (Hiro. Univ.) | H-4 | 1314 | 4-01 | H.4 | 27.038631 | -179.680471 |
| H | N.U.E. | H.U.P.S. (Hiro. Univ.) | H-5 | 1335 | 4-03 | H.5 | 27.052429 | -179.699436 |
| H | N.U.E. | H.U.P.S. (Hiro. Univ.) | H-2 | 1277 | 4-07 | H.2 | 27.012202 | -179.651249 |
| H | N.U.E. | H.U.P.S. (Hiro. Univ.) | H-1 | 1268 | 4-08 | H.1 | 27.017030 | -179.639148 |
| H | N.U.E. | H.U.S. (Hiro. Univ.) | HP-1 (H-1) | 1259 | 4-08 | H.1 | 27.017030 | -179.639148 |
| H | N.U.E. | H.U.P.S. (Hiro. Univ.) | H-3 | 1295 | 4-19 | H.3 | 27.031415 | -179.662921 |
| H | N.U.E. | Red Cross Hospital | HP-5 | 1433 | 5-01 | H.1 | 26.704789 | -179.850980 |
| H | N.U.E. | Chokin-Kyoku (Postal Savings) | | 1590 | 6-14 | 5 | 26.815913 | -179.994000 |
| H | N.U.E. | Denki keiki kentaisho | HP-6 | 1801 | 7-01 | C | 26.613600 | -176.610600 |
| H | N.U.E. | H.U.T. (Hiro. Univ) | HP-7 | 2036 | 8-01 | 2 | 26.808694 | -180.448681 |
| H | N.U.E. | Kirihara | KI-1 | 2453 | | | | |
| H | N.U.E. | Kirihara | KI-2 | 2453 | | | | |
| H | N.U.E. | Kirihara | KI-3 | 2453 | | | | |
| H | N.U.E. | Kirihara | KI-4 | 2453 | | | | |
| H | N.U.E. | Meisen -ji "Oni-gawara" | Me-1 | 1909 | | | | |
| H | N.U.E. | Meisen -ji "Oni-gawara" bottom | Hr-1 | 2053 | | | | |
| H | N.U.E. | Meisen -ji "Oni-gawara" top | Me-2 | 1909 | | | | |
| H | U.OF U. | H.U.F.S. (Hiro. Univ.) | UHFS01 | 1426 | 3-21 | H.26 | 27.086414 | -179.783523 |
| H | U.OF U. | H.U.F.S. (Hiro. Univ.) | UHFS02 | 1396 | 3-22 | H.7 | 27.069449 | -179.755880 |
| H | U.OF U. | H.U.F.S. (Hiro. Univ.) | UHFS03 | 1389 | 3-23 | H.24 | 27.082903 | -179.748183 |
| H | U.OF U. | H.U.F.S. (Hiro. Univ.) | UHFS04 | 1451 | 3-24 | H.28 | 27.067298 | -179.817963 |
| H | U.OF U. | H.U.F.S. (Hiro. Univ.) | UHFS05 | 1430 | 3-25 | H.27 | 27.057379 | -179.795993 |
| H | U.OF U. | H.U.F.S. (Hiro. Univ.) | UHFS06 | 1455 | 3-26 | H.32 | 27.098598 | -179.813883 |
| H | U.OF U. | H.U.F.S. (Hiro. Univ.) | UHFS07 | 1454 | 3-27 | H.3 | 27.098000 | -179.813000 |
| H | U.OF U. | H.U.F.S. (Hiro. Univ.) | UHFSFT01 | 1433 | 3-35 | H.29 | 27.102843 | -179.801165 |
| N | J.N.I.R.S. | Ieno | A,B | 1427 | N-2 | 3-1 | 34.135000 | -23.967000 |
| N | J.N.I.R.S. | Inasa | A | 2026 | N-3 | 5-1 | 34.416000 | -27.436500 |
| N | J.N.I.R.S. | Urakami | | 459 | N-4 | 1 | 34.685500 | -25.111500 |
| N | J.N.I.R.S. | Sakamoto | | 1079 | N-6 | 2 | 34.721000 | -26.350000 |
| N | J.N.I.R.S. | Zenza | | 1437 | N-7 | 4 | 34.545000 | -26.789500 |
| N | J.N.I.R.S. | Chikugo | | 2369 | N-8 | 6 | 35.179000 | -27.527500 |
| N | J.N.I.R.S. | Ieno | C | 1437 | | 3-2 | 34.147500 | -23.964000 |
| N | J.N.I.R.S. | Inasa | B | 2026 | | 5-2 | 34.411030 | -27.438860 |
| N | J.N.I.R.S. | Inasa | C | 2026 | | 5-3 | 34.411030 | -27.438860 |
| N | J.N.I.R.S. | Inasa | D, E, F | 2030 | | 5-4 | 34.400495 | -27.450485 |
| N | N.U.E. | Brazier (Shioyama 1a) | | 836 | N-17 | N-17 | 33.521000 | -25.313500 |
| N | N.U.E. | Ieno wall | | 1427 | N-2 | N-2 | 34.135000 | -23.967000 |
| N | N.U.E. | Ceramic (Nishimachi 12d) | | 1127 | N-38 | N-38 | 33.752000 | -24.440000 |
| N | N.U.E. | Ieno roof tile | N-177 | 1800 | | N-18 | 34.241500 | -23.830000 |
| N | U. of U. | Ieno wall | NAIE | 1427 | N-2 | N-2 | 34.135000 | -23.967000 |

* Distance indicated by laboratory in appendix or previous publications

(Hiroshima) New Map Hypocenter 26.73500 x -178.3995 (Army Map Hypocenter 44.298 x 61.707) Ht. 580m

(Nagasaki) New Map Hypocenter 34.2475 x -25.3945 (Army Map Hypocenter 93.624 x 65.936) Ht. 503m

Table 1. Continued

| New Map Dist. (m) | ARMY MAP COORDINATE | | Army Map Dist. (m) | Δ Ol - NEW * (m) | Δ NEW - OLD (m) |
|---|---|---|---|---|---|
| 506.844 | 44.722308 | 61.347593 | 508.468 | 8.2 | -1.6 |
| 523.065 | 44.718540 | 61.309507 | 529.132 | 15.9 | -6.1 |
| 3132.700 | | | 0.000 | | |
| 621.011 | 44.968596 | 61.618483 | 618.512 | 0.0 | 2.5 |
| 665.365 | 44.955934 | 60.973361 | 672.928 | -5.4 | -7.6 |
| 691.794 | 44.948279 | 60.948559 | 695.041 | -11.8 | -3.2 |
| 1456.854 | 44.648776 | 60.158178 | 1452.110 | -13.9 | 4.7 |
| 1376.955 | 44.614946 | 60.240362 | 1372.052 | -11.0 | 4.9 |
| 1387.374 | 44.582023 | 60.221690 | 1382.776 | -19.4 | 4.6 |
| 1428.392 | 44.609712 | 60.183331 | 1422.100 | -0.4 | 6.3 |
| 1400.738 | 44.596015 | 60.209507 | 1396.160 | -7.7 | 4.6 |
| 1424.925 | 44.592131 | 60.183136 | 1419.140 | -8.9 | 5.8 |
| 1426.082 | 44.629915 | 60.189760 | 1420.174 | -6.1 | 5.9 |
| 1451.794 | 44.227492 | 60.123184 | 1449.676 | -18.8 | 2.1 |
| 1131.154 | 45.538000 | 61.778000 | 1135.713 | 8.8 | -4.6 |
| 523.415 | 44.705889 | 61.300895 | 526.312 | -8.4 | -2.9 |
| 691.794 | 44.348279 | 60.948559 | 695.041 | -11.8 | -3.2 |
| 1378.438 | 44.610333 | 60.237746 | 1373.506 | -9.4 | 4.9 |
| 1388.475 | 44.578974 | 60.219961 | 1383.808 | -12.5 | 4.7 |
| 1450.522 | 44.640807 | 60.165286 | 1444.173 | -1.5 | 6.3 |
| 1460.942 | 44.610599 | 60.145475 | 1456.188 | -0.9 | 4.8 |
| 1427.936 | 44.596643 | 60.180633 | 1422.174 | -1.9 | 5.8 |
| 1421.984 | 44.616936 | 60.192143 | 1415.553 | -1.0 | 6.4 |
| 1387.908 | 44.605734 | 60.225078 | 1383.978 | -0.9 | 3.9 |
| 1387.908 | 44.605734 | 60.225078 | 1383.978 | -10.9 | 3.9 |
| 1449.128 | 44.638730 | 60.164108 | 1444.814 | | 4.3 |
| 1393.097 | 44.608751 | 60.216730 | 1392.013 | 3.9 | 1.1 |
| 1316.464 | 44.586640 | 60.290712 | 1321.675 | -2.5 | -5.2 |
| 1338.131 | 44.604900 | 60.263900 | 1349.081 | -3.1 | -10.9 |
| 1282.075 | 44.548001 | 60.336375 | 1273.977 | -5.1 | 8.1 |
| 1271.325 | 44.556718 | 60.347978 | 1265.007 | -3.3 | 6.3 |
| 1271.325 | 44.556718 | 60.347978 | 1265.007 | -12.3 | 6.3 |
| 1297.727 | 44.576214 | 60.314766 | 1298.229 | -2.7 | -0.5 |
| 1451.794 | 44.227492 | 60.123184 | 1449.676 | -18.8 | 2.1 |
| 1596.552 | | | 0.000 | -6.6 | |
| 1793.015 | | | 0.000 | 8.0 | |
| 2050.506 | 44.310390 | 59.469413 | 2046.081 | -14.5 | 4.4 |
| ******* | 741.730000 | 1261.050000 | 0.000 | | |
| ******* | 741.730000 | 1261.050000 | 0.000 | | |
| ******* | 741.730000 | 1261.050000 | 0.000 | | |
| ******* | 741.730000 | 1261.050000 | 0.000 | | |
| ******* | 746.290000 | 1261.080000 | 0.000 | | |
| ******* | 742.150000 | 1261.050000 | 0.000 | | |
| ******* | 746.290000 | 1261.080000 | 0.000 | | |
| 1427.940 | 44.624776 | 60.186846 | 1421.782 | -1.9 | 6.2 |
| 1397.005 | 44.608751 | 60.216730 | 1392.013 | -1.0 | 5.0 |
| 1392.832 | 44.619212 | 60.222663 | 1388.694 | -3.8 | 4.1 |
| 1456.866 | 44.604867 | 60.148930 | 1452.069 | -5.9 | 4.8 |
| 1433.220 | 44.593621 | 60.173858 | 1427.728 | -3.2 | 5.5 |
| 1460.371 | 44.637016 | 60.151508 | 1455.731 | -5.4 | 4.6 |
| 1459.367 | 44.647469 | 60.157436 | 1452.509 | -5.4 | 6.9 |
| 1449.128 | 44.638730 | 60.164108 | 1444.814 | -16.1 | 4.3 |
| 1431.926 | 93.470000 | 67.500000 | 1437.038 | -4.9 | -5.1 |
| 2048.940 | 93.865000 | 63.712500 | 2045.076 | -22.9 | 3.9 |
| 521.472 | 94.081500 | 66.247000 | 505.844 | -62.5 | 15.6 |
| 1066.388 | 94.144000 | 64.888000 | 1069.771 | 12.6 | -3.4 |
| 1426.370 | 93.967000 | 64.407500 | 1432.419 | 10.6 | -6.0 |
| 2327.527 | 94.712000 | 63.614500 | 2344.345 | 41.5 | -16.8 |
| 1433.991 | 93.476000 | 67.502500 | 1438.706 | 3.0 | -4.8 |
| 2050.890 | 93.860660 | 63.709970 | 2046.953 | -24.9 | 3.9 |
| 2050.890 | 93.860660 | 63.709970 | 2046.953 | | 3.9 |
| 2061.670 | 93.850265 | 63.696310 | 2058.397 | | 3.3 |
| 731.002 | 92.808000 | 66.030000 | 751.085 | 105.0 | -20.1 |
| 1431.926 | 93.470000 | 67.500000 | 1437.038 | -4.9 | -5.1 |
| 1075.449 | 93.071000 | 66.992000 | 1089.996 | 51.6 | -14.5 |
| 1564.512 | 93.600000 | 67.643500 | 1561.492 | 35.5 | 3.0 |
| 1431.926 | 93.470000 | 67.500000 | 1437.038 | -4.9 | -5.1 |

structures and large objects was known.
7. Gamma-ray dosimetry of natural background could be carried out at the sample location.

Two kinds of ground distances are given in Table 1, one based on army maps and the other on a new map. The army maps were prepared in the period 1945-46 by the US Army Map Service, with coordinate units of 1000 yards. The new maps are based on surveys in 1979 (Hiroshima) and 1981 (Nagasaki) and published by the two cities. The scale is 1/2500 with coordinate units of 1000 m. To relate locations on the new and old maps, a new map was placed on an old map of the same scale, matched at existing fixed points, and the hypocenter on the old map transferred to the new one.

**Sample Preparation.** The goals of sample preparation for A-bomb dosimetry are fourfold:

1. To isolate a TL material of sufficient sensitivity to allow measurement of the doses of interest.
2. To provide a homogeneous material with respect to TL output, avoiding competing TL components from unwanted minerals.
3. To provide a homogeneous TL material which had experienced throughout, as closely as possible, the same radiation history with respect to alpha, beta, gamma, cosmic, and A-bomb radiation.
4. To accomplish this without increasing, decreasing, or introducing spurious components into the TL signal.

In TL dosimetry using contemporary ceramic materials the two most often used methods of analysis are the quartz inclusion technique[12] and the pre-dose technique.[13] The fine grain technique,[14] which is commonly used for dating archaeological samples, has not proven useful for low-dose environmental samples.[15]

All preparation techniques begin by removing several millimeters of material from the outer surface of the potsherd, brick, tile, etc. The purpose of the removal is to improve uniformity of dose since, with the limited range of beta particles within a sample, a pronounced drop-off in the dose often occurs at the edge of the ceramic. Removing a portion of sample roughly equivalent to the range of the particles produced in the sample (2 to 3 mm) insures that the portion to be used for analysis has been exposed to a beta particle field unaffected by edge effects. Removing several millimeters of outer surface also, in the case of impinging gamma radiation, removes the electron buildup material which would have experienced lower levels of radiation than the remainder of the sample. The removal of this portion is usually accomplished with a water cooled lapidary saw, but surface grinding is common for nonflat and textured surfaces.

In addition to removal of the outer portion of the sample, the quartz inclusion technique involves: (1) gentle crushing of the sample, (2) separation of particles by sifting, (3) elimination of clay-containing particles using magnetic separators, and (4) removal of nonquartz particles by acid treatment and/or heavy-liquid separation. Each of the steps may be followed by washing and drying of the sample in high purity acetone.

The net effect of the procedure is to: (1) provide a sample of maximal light output due to removal of non-TL emitting inclusions and surface quantities of clay and other opaque materials, (2) remove competing TL producing minerals, and (3) provide a sample with nearly uniform radiation history and beta-particle attenuation by sizing and removal of clay. Uniformity is further addressed by allowing the sample to remain in hydrofluoric acid for sufficient time to remove approximately 6 $\mu$m from its surface. Etching has the desired effect of removing that component of the sample which had been exposed to radiation from alpha particles originating within the clay matrix. As the alpha-particle component of dose-rate becomes negligible the formula for dosimetry with the quartz inclusion technique becomes:

$$D = TL - A(\beta + \gamma + c) \tag{5}$$

The removal also reduces the component of dose due to radiation originating within the sample while increasing the fractional dose due to external radiation.

**High Temperature Analysis**

Samples yielding dose estimates for Hiroshima and Nagasaki were analyzed with variations of the quartz inclusion technique and variations of the pre-dose technique. Because prepared samples have ranged from slices of tile to quartz inclusions to heterogeneous powders, the term "high temperature analysis" rather than the more preparation-specific term "quartz inclusion technique" will be used henceforth in this report. This is the procedure that gives the glow curves described in the introduction.

**Stability of Thermoluminescence (Plateau Test).** The first step in high temperature TL analysis involves determining the region of the TL glow curve that is free from fading effects. Fading falls into two categories, thermal fading and anomalous, or nonthermal, fading. The first category, described by Equation (1), is a function of trap depth and does not occur at higher temperatures on the glow curve. The second category, anomalous fading, typically occurs over the first few hours or days only and may affect peaks at any temperature. Hashizume et al[2] identified and described a typical case of anomalous fading in their powdered TL samples from Hiroshima and Nagasaki.

To detect the regions of the glow curve free from fading, the "plateau test" is performed. The test involves the comparison of two glow curves from the same sample. The first is a glow curve of the dose being measured (a), the second a glow curve of a dose subsequently applied in the laboratory (b). The temperature regions which show equivalent TL ratios (Figure 8) are assumed to be free of fading.

Anomalous fading, not seen in the 375°C TL region of quartz, but common in zircon and many feldspars, is usually also detected with the plateau test. Occasionally, however, an extended high temperature region of the glow curve will be affected uniformly by anomalous fading, and the plateau test will falsely indicate a region of stability. Anomalous fading is best detected by irradiating an annealed sample and measuring the TL output over a period of months. By so doing a correction factor for the dose estimate may be obtained, similar to that derived by Hashizume et al.[2]

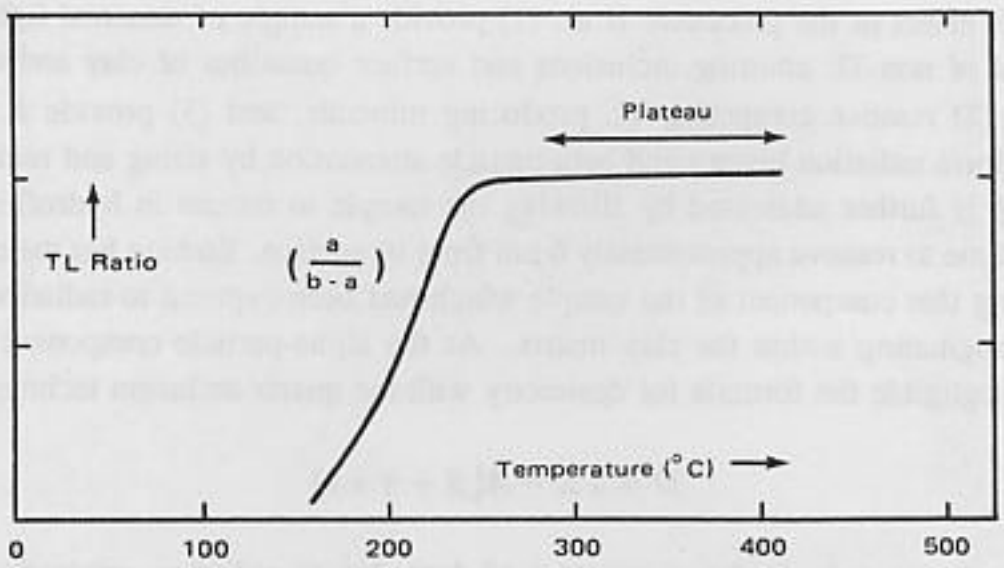


*Figure 8. The plateau test.*

**Historical Methods (Curve Matching).** Curve matching is the simplest form of high temperature TL analysis. It is of interest here since many contemporary TL techniques have been developed to circumvent shortcomings of curve matching and also because it was the technique used previously on Hiroshima and Nagasaki samples.[1,2]

To obtain an estimate of the dose using curve-matching procedures, a glow curve ($TL_N$) is taken in which the sample is heated to 400 to 500 °C. After cooling, the sample is given a calibrating dose of radiation (B) and another glow curve ($TL_B$) is obtained by the same heating cycle. If $TL_N$ and $TL_B$ are equal in the stable region, the dose is taken to be equal to the calibrating dose. If they are unequal, the dose is calculated by:

$$D = (TL_N - TL_P) / (TL_B - TL_P) \tag{6}$$

where $TL_P$ is the photon emission due to the red-hot glow of the sample. The $TL_P$ glow must be corrected for when dealing with glow peaks whose tail continues into the incandescent region.

This technique works well under controlled conditions. A modification was used for determining dose-rate effects and for interlaboratory calibrations (Appendix 4-10). However this method often fails for two reasons:

1. Supralinearity. At low doses the TL output per unit dose for many phosphors, including quartz, is small but increases gradually with increasing dose (supralinearity) until a linear region is obtained (Figure 9). At much higher doses saturation effects lead to sublinearity. In a perfectly behaved quartz crystal displaying only supralinearity, the dose could be determined by curve matching if the glow curve closely matched that of the calibrating dose. Equation (6) fails, however, for $TL_B \neq TL_N$. Unfortunately, it is impossible to know if a sample is well behaved without first performing a variety of diagnostic tests.
2. Sensitivity Change. A second phenomenon, common in feldspars and in the 325 °C

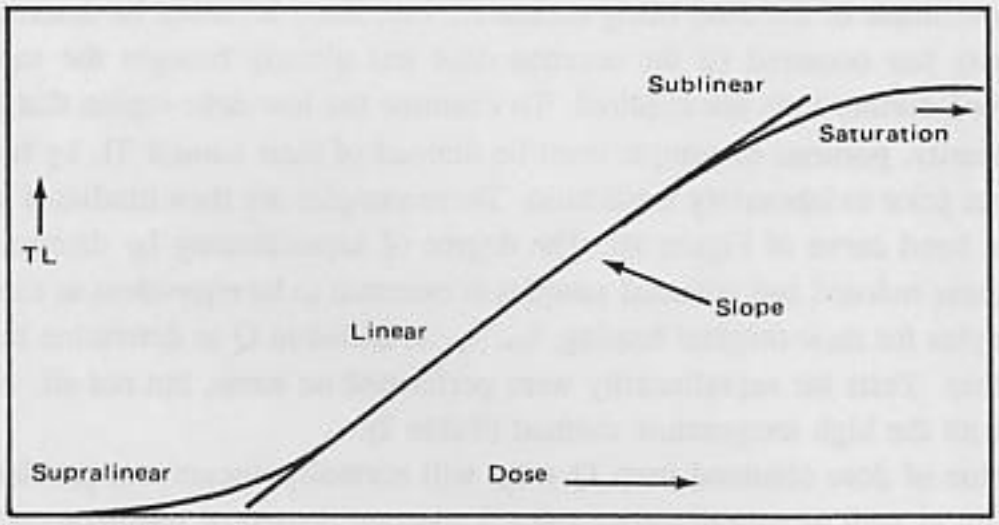


*Figure 9. Linearity and nonlinearity.*

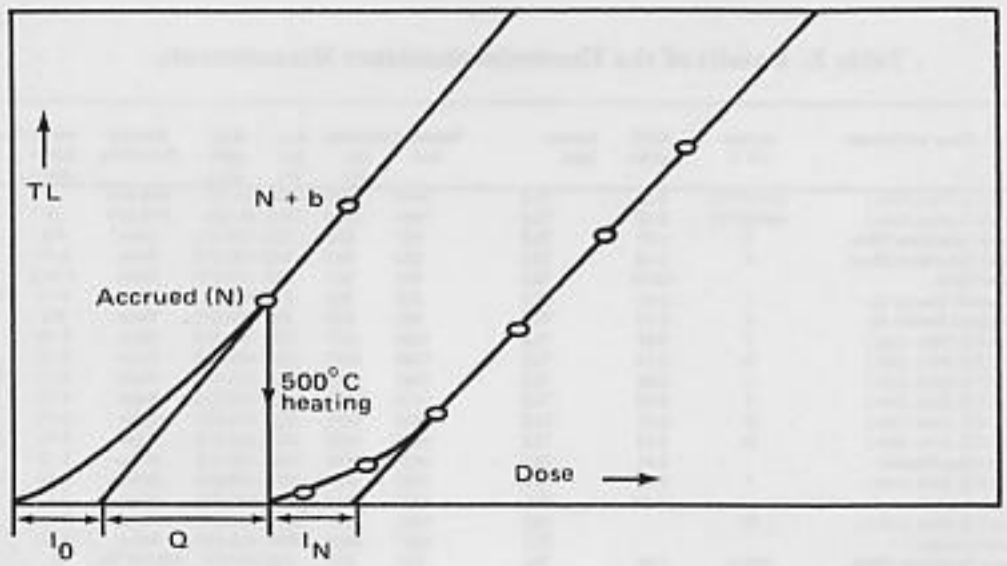


Supralinearity ($I_0$) associated with the accrued dose of a sample is deduced from the degree of supralinearity ($I_N$) measured in the same sample following annealing and redosing. The estimate of accrued dose to the sample is then $I_N + Q$, where Q is the estimate of dose uncorrected for supralinearity.

*Figure 10. Correction for supralinearity.*

peak of quartz, can preclude the use of curve matching altogether. The effect, a change in sensitivity following the first laboratory heating, typically results in an underestimate of the dose. Since the sensitivity change sometimes occurs following the first heating only, detection by curve matching may fail.

**The Additive Dose Method.** The additive dose technique, employed to overcome the problems of supralinearity and change in sensitivity, involves irradiating several portions of a sample with different doses in addition to the dose being measured. The light output from the sample is then plotted as a function of the added laboratory dose (Figure 10). Extrapolation back to the dose axis (Q in Figure 10) would, if supralinearity had not occurred,

provide an estimate of the dose being measured; but, since it cannot be determined whether supralinearity has occurred (if the accrued dose has already brought the sample into the linear region), further tests are required. To examine the low dose region that is susceptible to supralinearity, portions of sample must be drained of their natural TL by heating to high temperatures prior to laboratory irradiation. These samples are then irradiated and plotted as in the right hand curve of Figure 10. The degree of supralinearity $I_N$ determined from the curve for these redosed and reheated samples is assumed to be equivalent to that experienced by the samples for their original heating, $I_O$. $I_N$ is added to Q to determine the original (or accrued) dose. Tests for supralinearity were performed on some, but not all, of the samples analyzed with the high temperature method (Table 2).

The value of dose obtained from $Q + I_N$ will normally circumvent problems of change in sensitivity as well as supralinearity since a constant degree of sensitization will not alter the intercept value. In some conditions, particularly with samples containing feldspars, the change in sensitization is not constant, but varies with dose. Fleming[16] proposed a method

**Table 2. Results of the Thermoluminescence Measurements.**

| City | Lab. | Place and Sample | Sample I.D. # | RERF List No. | Sample Type | Reported Dist | NewMap Dist (m) | Army Dist (m) | Grain diam. (μm) | Etching Procedure | Samp. Depth (mm) | Shield | *TL Method | Plat Test |
|---|---|---|---|---|---|---|---|---|---|---|---|---|---|---|
| H | DUR | H.U.F.S. (Hiro. Univ.) | UHFSFT02 | 3-35 | TILE | 1454 | 1449 | 1445 | 90-150 | HFS 24hr | 3- | | HT | |
| H | DUR | H.U.F.S. (Hiro. Univ.) | UHFSFT02 | 3-35 | TILE | 1454 | 1449 | 1445 | 90-150 | HFS 24hr | 3- | | PD M.A.D. | |
| H | J.N.I.R.S. | Naka Telephone Office | 3 | 1-01 | TILE | 507 | 507 | 508 | 105-210 | None | 4-9 | | HT | Y |
| H | J.N.I.R.S. | Naka Telephone Office | 2 | 1-19 | TILE | 523 | 523 | 529 | 105-210 | None | 6-13 | | HT | Y |
| H | J.N.I.R.S. | Sanin Bank | | 12-02 | TILE | 621 | 621 | 619 | 105-210 | None | 4-10.5 | | HT | Y |
| H | J.N.I.R.S. | Chugoku Electric Co | 1 | 2-01 | TILE | 665 | 665 | 673 | 105-210 | None | 4-10 | S | HT | Y |
| H | J.N.I.R.S. | Chugoku Electric Co | 2 | 2-03 | TILE | 691 | 692 | 695 | 105-210 | None | 4-8 | | HT | Y |
| H | J.N.I.R.S. | H.U.F.S. (Hiro. Univ.) | 7 | 3-07 | TILE | 1366 | 1377 | 1372 | 105-210 | None | 5-15 | | PD | |
| H | J.N.I.R.S. | H.U.F.S. (Hiro. Univ.) | 10 | 3-10 | TILE | 1368 | 1387 | 1383 | 105-210 | None | 5-15 | | PD | |
| H | J.N.I.R.S. | H.U.F.S. (Hiro. Univ.) | I | 3-28 | TILE | 1393 | 1401 | 1396 | 105-210 | None | 5-15 | S | PD | |
| H | J.N.I.R.S. | H.U.F.S. (Hiro. Univ.) | II | 3-29 | TILE | 1416 | 1425 | 1419 | 105-210 | None | 5-15 | | PD | |
| H | J.N.I.R.S. | H.U.F.S. (Hiro. Univ.) | IV | 3-31 | TILE | 1420 | 1426 | 1420 | 105-210 | None | 5-15 | | PD | |
| H | J.N.I.R.S. | H.U.F.S. (Hiro. Univ.) | 14 | 3-14 | TILE | 1428 | 1428 | 1422 | 105-210 | None | 5-15 | S | PD | |
| H | J.N.I.R.S. | Red Cross Hospital | | 5-01 | TILE | 1433 | 1452 | 1450 | 105-210 | None | 5-15 | | PD | |
| H | J.N.I.R.S. | H.U.F.S. (Hiro. Univ.) | 1 | 3-01 | TILE | 1443 | 1457 | 1452 | 105-210 | None | 5-15 | S | PD | |
| H | J.N.I.R.S. | Ryomatsu-sho | | 11-04 | BRK | 3087 | 3133 | 0 | 105-210 | None | 5-15 | | PD | |
| H | J.N.I.R.S. | H.U.F.S. (Hiro. Univ.) | RI | | TILE | 1450 | #N/A | #N/A | 105-210 | None | 5-15 | | PD | |
| H | J.N.I.R.S. | Chokin-Kyoku | | | TILE | 1607 | #N/A | #N/A | 105-210 | None | 5-15 | | PD | |
| H | N.U.E. | Naka Telephone Office | 203-3 | 1-04 | Tile | 523 | 523 | 526 | 50-150 | 10% HF 1hr | 2- | | HT | Y |
| H | N.U.E. | Naka Telephone Office | 204-2 | 1-04 | Tile | 523 | 523 | 526 | 50-150 | 10% HF 1hr | 2- | | HT | Y |
| H | N.U.E. | Naka Telephone Office | 204-3 | 1-04 | Tile | 523 | 523 | 526 | 50-150 | 10% HF 1hr | 2- | | HT | Y |
| H | N.U.E. | Chugoku Electric Co. | 3-1-3 | 2-03 | Wall Tile | 692 | 692 | 695 | 50-75 | 10% HF 1hr | 2-11 | | HT | Y |
| H | N.U.E. | Chugoku Electric Co. | 3-1-3 | 2-03 | Wall Tile | 692 | 692 | 695 | 50-75 | 10% HF 1hr | 2-11 | | HT | Y |
| H | N.U.E. | Chugoku Electric Co. | 3-2-2 | 2-03 | Wall Tile | 692 | 692 | 695 | 50-75 | 10% HF 1hr | 2-11 | | HT | Y |
| H | N.U.E. | Chugoku Electric Co. | 3-2-2 | 2-03 | Wall Tile | 692 | 692 | 695 | 50-75 | 10% HF 1hr | 2-11 | | HT | Y |
| H | N.U.E. | Chugoku Electric Co. | 3-2-3 | 2-03 | Wall Tile | 692 | 692 | 695 | 50-150 | 10% HF 1hr | 2-11 | | HT | Y |
| H | N.U.E. | H.U.P.S. (Hiro. Univ.) | H-1 | 4-08 | Tile, railing | 1271 | 1271 | 1265 | 74-150 | 10% HF 1hr | 2-24 | | HT | Y |
| H | N.U.E. | HUFS "I" Bldg | HI | 4-08 | tile, railing, roof | 1271 | 1271 | 1265 | 74-150 | None | 2-24 | | PD MA | |
| H | N.U.E. | H.U.P.S. (Hiro. Univ.) | H-3 | 4-09 | Tile, railing | 1298 | 1271 | 1265 | 74-150 | 10% HF 1hr | 2-24 | | HT | Y |
| H | N.U.E. | H.U.P.S. (Hiro. Univ.) | H-2 | 4-07 | Tile, eaves | 1282 | 1282 | 1274 | 74-150 | 10% HF 1hr | 2-24 | | HT | Y |
| H | N.U.E. | H.U.P.S. (Hiro. Univ.) | H-4 | 4-01 | Tile, eaves | 1316 | 1316 | 1322 | 74-150 | 10% HF 1hr | 2-24 | | HT | Y |
| H | N.U.E. | H.U.P.S. (Hiro. Univ.) | H-5 | 4-03 | Tile, railing | 1338 | 1338 | 1349 | 74-150 | 10% HF 1hr | 2-24 | | HT | Y |
| H | N.U.E. | H.U.F.S. (Hiro. Univ.) | H-6-1 | 3-20 | Tile, floor | 1388 | 1388 | 1384 | 50-74 | 10% HF 1hr | 2-18 | | HT | Y |
| H | N.U.E. | H.U.F.S. (Hiro. Univ.) | H-6-2 | 3-20 | Tile, floor | 1388 | 1388 | 1384 | 50-74 | 10% HF 1hr | 2-18 | | HT | Y |
| H | N.U.E. | H.U.F.S. (Hiro. Univ.) | H-6-3 | 3-20 | Tile, floor | 1388 | 1388 | 1384 | 50-74 | 10% HF 1hr | 2-18 | | HT | Y |
| H | N.U.E. | H.U.F.S. (Hiro. Univ.) | H-7 | 3-36 | Tile, railing | 1393 | 1393 | 1392 | 50-74 | 10% HF 1hr | 2- | | HT | Y |
| H | N.U.E. | H.U.F.S. (Hiro. Univ.) | H-8 | 3-18 | Tile, floor | 1422 | 1422 | 1416 | 50-74 | 10% HF 1hr | 2- | | HT | Y |
| H | N.U.E. | H.U.F.S. (Hiro. Univ.) | H-9 | 3-17 | Tile, floor | 1428 | 1428 | 1422 | 50-74 | 10% HF 1hr | 2- | | HT | Y |
| H | N.U.E. | H.U.F.S. (Hiro. Univ.) | H-10-1 | 3-15 | Tile, floor | 1451 | 1451 | 1444 | 50-74 | 10% HF 1hr | 2- | | HT | Y |
| H | N.U.E. | H.U.F.S. (Hiro. Univ.) | H-10-2 | 3-15 | Tile, floor | 1451 | 1451 | 1444 | 50-74 | 10% HF 1hr | 2- | | HT | Y |
| H | N.U.E. | H.U.F.S. (Hiro. Univ.) | H-10-3 | 3-15 | Tile, floor | 1451 | 1451 | 1444 | 50-74 | 10% HF 1hr | 2- | | HT | Y |
| H | N.U.E. | H.U.F.S. (Hiro. Univ.) | H-10-4 | 3-15 | Tile, floor | 1451 | 1451 | 1444 | 50-74 | 10% HF 1hr | 2- | | HT | Y |
| H | N.U.E. | H.U.F.S. (Hiro. Univ.) | H-11 | 3-16 | Tile, floor | 1461 | 1461 | 1456 | 50-74 | 10% HF 1hr | 2- | | HT | Y |
| H | N.U.E. | Japanese House (Nobori-cho) | | | Ora-gawara | 1131 | #N/A | #N/A | 50-150 | 10% HF 1hr | 2- | | HT | Y |
| H | N.U.E. | HUFS "I" Bldg | HS-B | | tile, raising, roof | 1298 | #N/A | #N/A | 50-150 | None | 2-24 | ertical si | PD MA | |
| H | N.U.E. | HUFS "E" Bldg | HP1 | | tile, wall | 1378 | #N/A | #N/A | 74-150 | None | 2-18 | | PD MA | |
| H | N.U.E. | HUFS "E" Bldg | HP2 | | tile, raising, roof | 1388 | #N/A | #N/A | 74-150 | None | 2-18 | | PD MA | |
| H | N.U.E. | HUFS "E" Bldg | HP3 | | tile, wall | 1388 | #N/A | #N/A | 74-150 | None | 2-18 | | PD MA | |
| H | N.U.E. | Red Cross Hospital | HP4 | | tile, floor of roof | 1451 | #N/A | #N/A | 74-150 | None | 2- | | PD MA | |
| H | N.U.E. | Chokin-Kyoku (Postal Savings) | | | R Tile | 1597 | #N/A | #N/A | 50-150 | 10% HF 1hr | 2- | | HT | Y |
| H | N.U.E. | Mesen -ji "Ora-gawara" top | Me-1 | | Roof Ornment | 1909 | #N/A | #N/A | 74-150 | 10%HF 1hr | 1- | | HT | Y |
| H | N.U.E. | Mesen -ji "Ora-gawara" bottom | Me-2 | | Roof Ornment | 1909 | #N/A | #N/A | 74-150 | 10%HF 1hr | 1- | | HT | Y |
| H | N.U.E. | HUFE | HP5 | | tile, wall | 2041 | #N/A | #N/A | 74-150 | None | 2- | | PD MA | |
| H | N.U.E. | Hiramoto"Ora-gawara" bottom | Hr-1 | | Roof Ornment | 2053 | #N/A | #N/A | 74-150 | 10%HF 1hr | 1- | | HT | Y |
| H | N.U.E. | Kinhara | Ki-1 | | roof tile | 2453 | #N/A | #N/A | 74-150 | 10%HF 1hr | 1- | | HT | Y |
| H | N.U.E. | Kinhara | Ki-2 | | roof tile | 2453 | #N/A | #N/A | 74-150 | 10%HF 1hr | 1- | | HT | Y |

of correcting for this type of change, assuming a linear change in sensitization occurred with dose. Bowman,[17] however, demonstrated that it was infeasible in practice. Therefore, samples showing changes in sensitization as a function of dose are best discarded.

The first step in the test is to determine whether any change in sensitivity has occurred as a result of the first heating. This is done by comparing the slopes of the first glow heatings with those of the second glow samples. If the slopes are parallel, then no change in sensitivity following the first heating has occurred. If the slopes are not parallel, then a change in sensitization is assumed to have occurred.

The test for determining whether or not the sensitization is dose-dependent is identical to the test just described for supralinearity, with the exception that the samples used to generate the second curve (right hand curve of Figure 11) are given a dose ($b_o$) in addition to the accrued dose prior to annealing and retesting. A difference of 20 % between the $I_N$ obtained with these two procedures is usually taken as an indication that the supralinearity is dose-dependent. Bailiff (Appendix 4-7) performed these measurements on quartz from tile

Table 2. Continued

| Supra Linear | Slope Ratios | Fading Test | Gross TL Dose (Gy) | ± (Gy) | Beta mGy/yr | B Atten | ± mGy/yr | Gamma mGy/yr | ± mGy/yr | Age (yr) | ± (yr) | Total Bkg Dose (Gy) | ± (Gy) | Net (Gy) | ± (Gy) | Dose to: (Gy) | Dose to Quartz Net (Gy) | Net Adjust** (Gy) | ± (Gy) | Gross Adjust** (Gy) | ± (Gy) |
|---|---|---|---|---|---|---|---|---|---|---|---|---|---|---|---|---|---|---|---|---|---|
| 4 | 0.60 | Y | 0.77 | 0.1 | 2.1 | 0.92 | 0.2 | 1.15 | 1 | 52 | 2 | 0.160 | 0.059 | 0.61 | 0.11 | quartz | 0.61 | 0.66 | 0.12 | 0.84 | 0.10 |
| | | | 0.78 | 0.1 | 2.1 | 0.92 | 0.2 | 1.15 | 1 | 52 | 2 | 0.160 | 0.059 | 0.62 | 0.11 | quartz | 0.62 | 0.68 | 0.12 | 0.85 | 0.10 |
| 210 | | | 30.3 | 2.7 | | | | | | | | | | - | - | tissue | - | - | - | 27.75 | 2.47 |
| 290 | | | 33.3 | 1.7 | | | | | | | | | | - | - | tissue | - | - | - | 30.50 | 1.56 |
| 310 | | | 19.6 | 1.7 | | | | | | | | | | - | - | tissue | - | - | - | 17.95 | 1.56 |
| 130 | | | 8 | 1.1 | | | | | | | | | | - | - | tissue | - | - | - | 7.33 | 1.01 |
| 50 | | | 10.5 | 1.7 | | | | | | | | | | - | - | tissue | - | - | - | 9.62 | 1.56 |
| | | | 1.15 | 0.1 | 2.65 | 1.00 | 0.32 | 1.25 | 0.04 | 52 | 2 | 0.203 | 0.020 | 0.95 | 0.07 | tissue | 0.87 | 0.87 | 0.07 | 1.05 | 0.06 |
| | | | 1.27 | 0.2 | 2.65 | 1.00 | 0.32 | 1.25 | 0.04 | 52 | 2 | 0.203 | 0.020 | 1.07 | 0.20 | tissue | 0.98 | 0.98 | 0.18 | 1.16 | 0.18 |
| | | | 0.11 | 0 | 2.65 | 1.00 | 0.32 | 1.25 | 0.04 | 52 | 2 | 0.203 | 0.020 | -0.09 | 0.03 | tissue | -0.08 | -0.08 | 0.03 | 0.10 | 0.02 |
| | | | 1.2 | 0.1 | 2.65 | 1.00 | 0.32 | 1.25 | 0.04 | 52 | 2 | 0.203 | 0.020 | 1.00 | 0.13 | tissue | 0.91 | 0.91 | 0.12 | 1.10 | 0.12 |
| | | | 0.97 | 0.1 | 2.65 | 1.00 | 0.32 | 1.25 | 0.04 | 52 | 2 | 0.203 | 0.020 | 0.77 | 0.05 | tissue | 0.70 | 0.70 | 0.05 | 0.89 | 0.05 |
| | | | 0.14 | 0.1 | 2.65 | 1.00 | 0.32 | 1.25 | 0.04 | 52 | 2 | 0.203 | 0.020 | -0.06 | 0.05 | tissue | -0.06 | -0.06 | 0.05 | 0.13 | 0.05 |
| | | | 0.75 | 0.1 | 2.75 | 1.00 | 0.36 | 1.21 | 0.07 | 44 | 2 | 0.174 | 0.021 | 0.58 | 0.10 | tissue | 0.53 | 0.53 | 0.09 | 0.69 | 0.09 |
| | | | 0.2 | 0 | 2.65 | 1.00 | 0.32 | 1.25 | 0.04 | 52 | 2 | 0.203 | 0.020 | 0.00 | 0.04 | tissue | 0.00 | 0.00 | 0.04 | 0.18 | 0.04 |
| | | | 0.23 | 0.1 | 1.91 | 1.00 | 0.38 | 1.2 | 0.08 | 73 | 2 | 0.227 | 0.034 | 0.00 | 0.06 | tissue | 0.00 | 0.00 | 0.06 | 0.21 | 0.05 |
| | | | 1.23 | 0.2 | 2.65 | 1.00 | 0.32 | 1.25 | 0.04 | 52 | 2 | 0.203 | 0.020 | 1.03 | 0.17 | tissue | 0.94 | 0.94 | 0.16 | 1.13 | 0.16 |
| | | | 0.52 | 0.1 | 2.96 | 1.00 | 0.45 | 1.25 | 0.09 | 47 | 2 | 0.198 | 0.027 | 0.32 | 0.07 | tissue | 0.30 | 0.30 | 0.06 | 0.48 | 0.05 |
| N | N | N | 32.5 | 2.9 | | | | | | | | | | - | - | Roentgen | - | - | - | 27.71 | 2.47 |
| N | N | N | 31 | 3.7 | | | | | | | | | | - | - | Roentgen | - | - | - | 26.43 | 3.15 |
| N | N | N | 30.5 | 4.4 | | | | | | | | | | - | - | Roentgen | - | - | - | 26.00 | 3.75 |
| N | N | N | 12.81 | 1.5 | 2.64 | 1.00 | 10 | 1.1 | 10 | 55 | | 0.206 | | 12.60 | - | tissue | 11.54 | 11.31 | - | 11.50 | 1.35 |
| N | N | N | 10.89 | 0.9 | 2.64 | 1.00 | 10 | 1.1 | 10 | 55 | | 0.206 | | 10.68 | - | tissue | 9.78 | 9.59 | - | 9.77 | 0.76 |
| N | N | N | 11.04 | 0.7 | 2.81 | 1.00 | 10 | 1.1 | 10 | 55 | | 0.215 | | 10.82 | - | tissue | 9.91 | 9.72 | - | 9.91 | 0.65 |
| N | N | N | 11.37 | 0.8 | 2.81 | 1.00 | 10 | 1.1 | 10 | 55 | | 0.215 | | 11.15 | - | tissue | 10.22 | 10.01 | - | 10.20 | 0.69 |
| N | N | N | 11.24 | 1.1 | 2.96 | 1.00 | 10 | 1.1 | 10 | 55 | | 0.223 | | 11.02 | - | Roentgen | 9.58 | 9.39 | - | 9.58 | 0.90 |
| 0 | N | N | 1.67 | 0.1 | 2.49 | 1.00 | 0.07 | 0.82 | 0.04 | 45 | 2 | 0.149 | 0.008 | 1.52 | 0.08 | Roentgen | 1.32 | 1.30 | 0.07 | 1.42 | 0.07 |
| | | | 1.98 | 0.1 | 2.49 | 1.00 | 0.07 | 0.82 | 0.04 | 45 | 2 | 0.149 | 0.008 | 1.83 | 0.11 | tissue | 1.68 | 1.64 | 0.10 | 1.78 | 0.10 |
| 0 | N | N | 1.68 | 0.2 | 2.49 | 1.00 | 0.07 | 0.82 | 0.04 | 45 | 2 | 0.149 | 0.008 | 1.53 | 0.22 | Roentgen | 1.33 | 1.31 | 0.19 | 1.43 | 0.19 |
| 0 | N | N | 1.72 | 0.2 | 2.49 | 1.00 | 0.07 | 0.82 | 0.04 | 45 | 2 | 0.149 | 0.008 | 1.57 | 0.15 | Roentgen | 1.37 | 1.34 | 0.13 | 1.47 | 0.13 |
| 0 | N | N | 1.34 | 0.3 | 2.49 | 1.00 | 0.07 | 0.82 | 0.04 | 45 | 2 | 0.149 | 0.008 | 1.19 | 0.25 | Roentgen | 1.04 | 1.02 | 0.21 | 1.14 | 0.21 |
| 0 | N | N | 1.22 | 0.2 | 2.49 | 1.00 | 0.07 | 0.82 | 0.04 | 45 | 2 | 0.149 | 0.008 | 1.07 | 0.16 | Roentgen | 0.93 | 0.91 | 0.14 | 1.04 | 0.14 |
| 0 | N | N | 1.09 | 0.2 | 2.71 | 1.00 | 0.07 | 0.88 | 0.03 | 52 | 2 | 0.187 | 0.009 | 0.90 | 0.17 | Roentgen | 0.79 | 0.77 | 0.15 | 0.93 | 0.14 |
| 0 | N | N | 1.07 | 0.1 | 2.71 | 1.00 | 0.07 | 0.88 | 0.03 | 52 | 2 | 0.187 | 0.009 | 0.88 | 0.05 | Roentgen | 0.77 | 0.75 | 0.04 | 0.91 | 0.04 |
| 0 | N | N | 1.17 | 0.1 | 2.71 | 1.00 | 0.07 | 0.88 | 0.03 | 52 | 2 | 0.187 | 0.009 | 0.98 | 0.06 | Roentgen | 0.86 | 0.84 | 0.05 | 1.00 | 0.05 |
| 0 | | | 1.02 | 0.1 | 2.71 | 1.00 | 0.07 | 0.88 | 0.03 | 52 | 2 | 0.187 | 0.009 | 0.83 | 0.12 | Roentgen | 0.72 | 0.71 | 0.10 | 0.87 | 0.10 |
| 0 | | | 0.94 | 0.1 | 2.71 | 1.00 | 0.07 | 0.88 | 0.03 | 52 | 2 | 0.187 | 0.009 | 0.75 | 0.06 | Roentgen | 0.66 | 0.64 | 0.05 | 0.80 | 0.05 |
| 0 | | | 0.85 | 0.1 | 2.71 | 1.00 | 0.07 | 0.88 | 0.03 | 52 | 2 | 0.187 | 0.009 | 0.66 | 0.06 | Roentgen | 0.58 | 0.57 | 0.05 | 0.72 | 0.05 |
| 0 | | | 1.01 | 0.1 | 2.71 | 1.00 | 0.07 | 0.88 | 0.03 | 52 | 2 | 0.187 | 0.009 | 0.82 | 0.13 | Roentgen | 0.72 | 0.70 | 0.11 | 0.86 | 0.11 |
| 0 | | | 0.96 | 0.1 | 2.71 | 1.00 | 0.07 | 0.88 | 0.03 | 52 | 2 | 0.187 | 0.009 | 0.77 | 0.07 | Roentgen | 0.67 | 0.66 | 0.06 | 0.82 | 0.06 |
| 0 | | | 0.89 | 0.1 | 2.71 | 1.00 | 0.07 | 0.88 | 0.03 | 52 | 2 | 0.187 | 0.009 | 0.70 | 0.11 | Roentgen | 0.61 | 0.60 | 0.09 | 0.76 | 0.09 |
| 0 | | | 0.96 | 0.1 | 2.71 | 1.00 | 0.07 | 0.88 | 0.03 | 52 | 2 | 0.187 | 0.009 | 0.77 | 0.07 | Roentgen | 0.67 | 0.66 | 0.06 | 0.82 | 0.06 |
| 0 | | | 0.7 | 0.1 | 2.71 | 1.00 | 0.07 | 0.88 | 0.03 | 52 | 2 | 0.187 | 0.009 | 0.51 | 0.06 | Roentgen | 0.45 | 0.44 | 0.05 | 0.60 | 0.05 |
| N | N | N | 2.02 | 0.1 | | | | | | | | | | - | - | Roentgen | - | - | - | 1.72 | 0.10 |
| | | | 1.16 | 0 | 2.37 | 1.00 | 0.07 | 0.78 | 0.04 | 45 | 2 | 0.142 | 0.800 | 1.02 | 0.80 | tissue | 0.93 | 0.91 | 0.72 | 1.04 | 0.01 |
| | | | 1.05 | 0.1 | 2.57 | 1.00 | 0.07 | 0.84 | 0.03 | 52 | 2 | 0.177 | 0.009 | 0.87 | 0.12 | tissue | 0.80 | 0.78 | 0.11 | 0.94 | 0.11 |
| | | | 1.11 | 0.1 | 2.57 | 1.00 | 0.07 | 0.84 | 0.03 | 52 | 2 | 0.177 | 0.009 | 0.93 | 0.08 | tissue | 0.85 | 0.84 | 0.07 | 1.00 | 0.07 |
| | | | 1.15 | 0.1 | 2.57 | 1.00 | 0.07 | 0.84 | 0.03 | 52 | 2 | 0.177 | 0.009 | 0.97 | 0.06 | tissue | 0.89 | 0.87 | 0.05 | 1.03 | 0.05 |
| | | | 0.83 | 0.1 | 3.29 | 1.00 | 1.06 | 1.16 | 10 | 45 | | 0.200 | | 0.63 | - | tissue | 0.58 | 0.57 | - | 0.74 | 0.10 |
| 5 | | | 0.58 | 0.1 | 3.23 | 1.00 | 0.32 | 0.82 | 0.04 | 40 | 2 | 0.162 | 0.017 | 0.42 | 0.06 | Roentgen | 0.36 | 0.36 | 0.05 | 0.49 | 0.05 |
| 0 | | | 0.37 | 0.1 | 1.1 | 1.00 | 10 | 1.4 | 10 | 71 | | 0.178 | | 0.19 | - | tissue | 0.18 | 0.17 | - | 0.33 | 0.07 |
| 0 | | | 0.36 | 0.1 | 1.1 | 1.00 | 10 | 1.4 | 10 | 71 | | 0.178 | | 0.18 | - | tissue | 0.17 | 0.16 | - | 0.32 | 0.07 |
| | | | 0.29 | 0.1 | 3.12 | | 10 | 0.96 | 10 | 55 | | 0.053 | | 0.24 | - | tissue | 0.22 | 0.21 | - | 0.26 | 0.04 |
| 4 | | | 0.22 | 0 | 2.4 | 1.00 | 10 | 1 | 10 | 48 | | 0.163 | | 0.06 | - | tissue | 0.05 | 0.05 | - | 0.20 | 0.04 |
| ? | | | 0.184 | 0 | 2.5 | 1.00 | 10 | 0.7 | 10 | 66 | | 0.211 | | -0.03 | - | tissue | -0.02 | -0.02 | - | 0.17 | 0.04 |
| ? | | | 0.113 | 0 | 1.1 | 1.00 | 10 | 1.3 | 10 | 66 | | 0.156 | | -0.05 | - | tissue | -0.04 | -0.04 | - | 0.10 | 0.02 |

Table 2. Continued

| City | Lab. | Place and Sample | Sample I.D. # | RERF List No. | Sample Type | Reported Dist | NewMap Dist (mi) | Army Dist (mi) | Grain diam. (μm) | Etching Procedure | Samp. Depth (mm) | Shield | *TL Method | Plat Test |
|---|---|---|---|---|---|---|---|---|---|---|---|---|---|---|
| H | N.U.E. | Kinhara | KI-3 | | roof tile | 2453 | #N/A | #N/A | 74-150 | 10%HF 1hr | 1- | | HT | Y |
| H | N.U.E. | Kinhara | KI-4 | | roof tile | 2453 | #N/A | #N/A | 74-150 | 10%HF 1hr | 1- | | HT | Y |
| H | OXF H | H.U.F.S. (Hiro. Univ.) | UHFSFT03 | 3-35 | TILE | 1454 | 1449 | 1445 | 90-125 | 40%HF 40 Min | 2- | | HT | Y |
| H | OXF S | H.U.F.S. (Hiro. Univ.) | UHFSFT03 | 3-35 | TILE | 1454 | 1449 | 1445 | Slice | None | 2- | | HT | Y |
| H | OXF S | H.U.F.S. (Hiro. Univ.) | UHFSFT03 | 3-35 | TILE | 1454 | 1449 | 1445 | Slice | None | 2- | | PD-MA | |
| H | U.OF U. | H.U.F.S. (Hiro. Univ.) | UHFS03 | 3-23 | TILE | 1396 | 1393 | 1389 | 106-150 | None | | | PD-MA | |
| H | U.OF U. | H.U.F.S. (Hiro. Univ.) | UHFS02 | 3-22 | TILE | 1426 | 1397 | 1392 | 106-150 | None | | | PD-MA | |
| H | U.OF U. | H.U.F.S. (Hiro. Univ.) | UHFS01 | 3-21 | TILE | 1433 | 1428 | 1422 | 106-150 & 150-250 | | | | | |
| H | U.OF U. | H.U.F.S. (Hiro. Univ.) | UHFS05 | 3-25 | TILE | 1451 | 1433 | 1428 | 106-150 | None | | S | PD-MA | |
| H | U.OF U. | H.U.F.S. (Hiro. Univ.) | UHFSFT02 | 3-35 | TILE | 1454 | 1449 | 1445 | Grains | None | | | PD-MA | |
| H | U.OF U. | H.U.F.S. (Hiro. Univ.) | UHFSFT03 | 3-35 | TILE | 1454 | 1449 | 1445 | Grains | None | | | PD-MA | |
| H | U.OF U. | H.U.F.S. (Hiro. Univ.) | UHFS04 | 3-24 | TILE | 1389 | 1457 | 1452 | 106-150 | None | | | PD-MA | |
| H | U.OF U. | H.U.F.S. (Hiro. Univ.) | UHFS07 | 3-27 | TILE | 1455 | 1459 | 1453 | Grains | None | | | PD-MA | |
| H | U.OF U. | H.U.F.S. (Hiro. Univ.) | UHFS06 | 3-26 | TILE | 1430 | 1460 | 1456 | 106-150 | None | | S | PD-MA | |
| N | Dur | leno wall | NAIEO6 | N-2 | Brick | 1427 | 1432 | 1437 | 90-150 | Conc HF 40m | 3-32 | | HT | Y |
| N | Dur | leno wall | NAIEO6 | N-2 | Brick | 1427 | 1432 | 1437 | 90-150 | Conc HF 40m | 34-64 | | HT | Y |
| N | Dur | leno wall | NAIEO6 | N-2 | Brick | 1427 | 1432 | 1437 | 90-150 | Conc HF 40m | 66-103 | | HT | Y |
| N | Dur | leno wall | NAIEO6 | N-2 | Brick | 1427 | 1432 | 1437 | 90-150 | Conc HFS 40h | 3-32 | | PD MA,MAD | |
| N | Dur | leno wall | NAIEO6 | N-2 | Brick | 1427 | 1432 | 1437 | 90-150 | Conc HFS 40h | 34-64 | | PD MA,MAD | |
| N | Dur | leno wall | NAIEO6 | N-2 | Brick | 1427 | 1432 | 1437 | 90-150 | Conc HFS 40h | 66-103 | | PD MA,MAD | |
| N | J.N.I.R.S. | Urakami | | N-4 | Brick | 459 | 521 | 506 | 105-210 | None | 5-15 | | HT | Y |
| N | J.N.I.R.S. | Sakamoto | | N-6 | Brick | 1079 | 1066 | 1070 | 105-210 | None | 5-15 | | HT | Y |
| N | J.N.I.R.S. | Zenze | | N-7 | Brick | 1437 | 1426 | 1432 | 105-210 | None | 5-15 | | PD | |
| N | J.N.I.R.S. | leno | A | N-2 | Brick | 1427 | 1432 | 1437 | 105-210 | None | 5-15 | | PD | |
| N | J.N.I.R.S. | leno | B | N-2 | Brick | 1427 | 1432 | 1437 | 105-210 | None | 5-15 | | PD | |
| N | J.N.I.R.S. | leno | C | N-2 | Brick | 1437 | 1432 | 1437 | 105-210 | None | 5-15 | S | PD | |
| N | J.N.I.R.S. | Inasa | A | N-3 | Brick | 2026 | 2049 | 2045 | 105-210 | None | 5-15 | | PD | |
| N | J.N.I.R.S. | Inasa | B | N-3 | Brick | 2026 | 2049 | 2045 | 105-210 | None | 5-15 | S | PD | |
| N | J.N.I.R.S. | Inasa | C | N-3 | Brick | 2026 | 2049 | 2045 | 105-210 | None | 5-15 | S | PD | |
| N | J.N.I.R.S. | Inasa | D | N-3 | Brick | 2036 | 2049 | 2045 | 105-210 | None | 5-15 | S | PD | |
| N | J.N.I.R.S. | Inasa | E | N-3 | Brick | 2036 | 2049 | 2045 | 105-210 | None | 5-15 | S | PD | |
| N | J.N.I.R.S. | Inasa | F | N-3 | Brick | 2036 | 2049 | 2045 | 105-210 | None | 5-15 | S | PD | |
| N | J.N.I.R.S. | Chikugo | | N-8 | Brick | 2369 | 2328 | 2344 | 105-210 | None | 5-15 | | PD | |
| N | N.U.E. | Brazier (Shirayama 1s) | | N-17 | Brazier | 731 | 731 | 751 | 50-150 | 10%HF 1hr | 2- | S | HT | |
| N | N.U.E. | leno roof tile | N-177 | N-18 | Roof tile | 1600 | 731 | 751 | 50-150 | 10%HF 1 hr | 2- | S | HT | |
| N | N.U.E. | Ceramic sherd | | N-38 | sherd | 1075 | 1075 | 1090 | 50-150 | 10%HF 1 hr | | S | HT | |
| N | N.U.E. | leno wall | A | N-2 | Brick | 1427 | 1432 | 1437 | 50-150 | 10%HF 1 hr | 2-36 | | HT | Y |
| N | N.U.E. | leno wall | B | N-2 | Brick | 1427 | 1432 | 1437 | 50-150 | 10%HF 1 hr | 36-70 | | HT | Y |
| N | N.U.E. | leno wall | C | N-2 | Brick | 1427 | 1432 | 1437 | 50-150 | 10%HF 1 hr | 70-104 | | HT | Y |
| N | Oxf H | leno wall | NAIEO6 | N-2 | Brick | 1427 | 1432 | 1437 | 90-125 | 40%HF 40 min | 3-32 | | HT | Y |
| N | Oxf H | leno wall | NAIEO6 | N-2 | Brick | 1427 | 1432 | 1437 | 90-125 | 40%HF 40 min | 34-64 | | HT | Y |
| N | Oxf H | leno wall | NAIEO6 | N-2 | Brick | 1427 | 1432 | 1437 | 90-125 | 40%HF 40 min | 66-103 | | HT | Y |
| N | U. of U. | leno wall | NAIEO6 | N-2 | Brick | 1427 | 1432 | 1437 | 150-250 | 48%HF 40min | 4-36 | | PD MA | |
| N | U. of U. | leno wall | NAIEO6 | N-2 | Brick | 1427 | 1432 | 1437 | 150-250 | 48%HF 40min | 37-69 | | PD MA | |
| N | U. of U. | leno wall | NAIEO6 | N-2 | Brick | 1427 | 1432 | 1437 | 150-250 | 48%HF 40min | 70-102 | | PD MA | |

* HT = High Temperature
PD = Pre-dose
MA = Pre-dose Multiple Activation Technique
MAD = Pre-dose Modified Additive Dose Technique
AD = Pre-dose Additive Dose Technique
HF = Hydrofluoric Acid
HFS = Hydrofluosilicic acid

** Correction factors based on intercalibration using NBS irradiated MSO

| | |
|---|---|
| DUR | 1.09 |
| J.N.I.R.S. | 1.00 |
| N.U.E. | 0.98 |
| OXF | 1.06 |
| U of U | 1.11 |

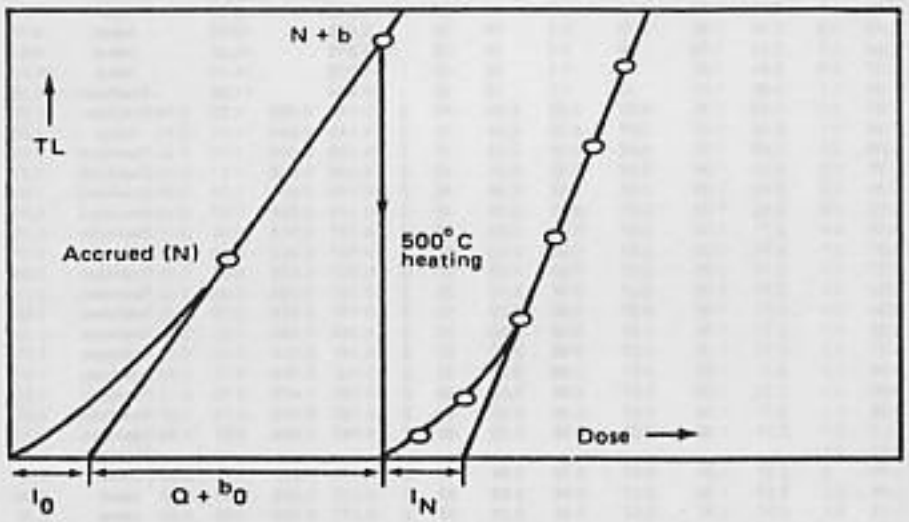


The test for dose-dependent supralinearity is made by measureing supralinearity in a sample after an additional dose has been added. If the resulting correction ($I_N$) is the same as that measured using the procedure of Figure 10, then the degree of supralinearity is assumed to be independent of dose.

*Figure 11. Correction for supralinearity with an added laboratory dose.*

Table 2. Continued

| Supra Linear | Slope Ratios | Fading Test | Gross TL Dose (Gy) | ± (Gy) | Beta mGy/yr | B Atten. | ± | Gamma mGy/yr | ± mGy/yr | Age (yr) | ± (yr) | Total Bkg Dose (Gy) | ± (Gy) | Net (Gy) | ± (Gy) | Dose to: | Dose to Quartz Net (Gy) | Net Adjust** (Gy) | ± (Gy) | Gross Adjust** (Gy) | ± (Gy) |
|---|---|---|---|---|---|---|---|---|---|---|---|---|---|---|---|---|---|---|---|---|---|
| ? | | | 0.192 | 0 | 1.7 | 1.00 | 10 | 1.3 | 10 | 66 | | 0.198 | | -0.01 | - | tissue | -0.01 | -0.01 | - | 0.17 | 0.03 |
| ? | | | 0.184 | 0 | 1.7 | 1.00 | 10 | 1.3 | 10 | 66 | | 0.198 | | -0.01 | - | tissue | -0.01 | -0.01 | - | 0.17 | 0.03 |
| 9 | | | 0.84 | 0.1 | 2.1 | 1.00 | 0.21 | 1.15 | 1 | 52 | 2 | 0.169 | 0.063 | 0.67 | 0.12 | quartz | 0.67 | 0.71 | 0.13 | 0.89 | 0.11 |
| N | | Y | 0.87 | 0.1 | 2.1 | 1.00 | 0.21 | 1.15 | 1 | 52 | 2 | 0.169 | 0.063 | 0.70 | 0.11 | quartz | 0.70 | 0.74 | 0.12 | 0.92 | 0.10 |
| | | | 0.87 | 0.1 | 2.3 | 1.00 | 0.46 | 1.15 | 1 | 52 | 2 | 0.179 | 0.076 | 0.69 | 0.10 | quartz | 0.69 | 0.73 | 0.11 | 0.92 | 0.07 |
| | | | 1.06 | 0 | 3.08 | 0.85 | 0.15 | 1.15 | 0.1 | 52 | 2 | 0.196 | 0.014 | 0.86 | 0.03 | quartz | 0.86 | 0.96 | 0.04 | 1.18 | 0.03 |
| | | | 1.1 | 0.1 | 3.08 | 0.85 | 0.15 | 1.15 | 0.1 | 52 | 2 | 0.196 | 0.014 | 0.90 | 0.07 | quartz | 0.90 | 1.00 | 0.08 | 1.22 | 0.08 |
| | | | 0.01 | 0 | 10 | | 10 | 10 | 10 | | | 0.000 | | - | - | quartz | - | - | - | 0.01 | 0.01 |
| | | | 0.14 | 0 | 3.08 | 0.85 | 0.15 | 1.15 | 0.1 | 52 | 2 | 0.196 | 0.014 | -0.06 | 0.02 | quartz | -0.06 | -0.06 | 0.02 | 0.16 | 0.01 |
| | | | 0.78 | 0.1 | 2 | 0.85 | 0.2 | 1.15 | 1 | 52 | 2 | 0.148 | 0.057 | 0.63 | 0.08 | quartz | 0.63 | 0.70 | 0.08 | 0.87 | 0.06 |
| | | | 0.74 | 0.1 | 2 | 0.85 | 0.2 | 1.15 | 1 | 52 | 2 | 0.148 | 0.057 | 0.59 | 0.10 | quartz | 0.59 | 0.66 | 0.11 | 0.82 | 0.09 |
| | | | 0.83 | 0 | 3.08 | 0.85 | 0.15 | 1.15 | 0.1 | 52 | 2 | 0.196 | 0.014 | 0.63 | 0.04 | quartz | 0.63 | 0.70 | 0.05 | 0.92 | 0.04 |
| | | | 0.67 | 0.1 | 3.08 | 0.85 | 0.15 | 1.15 | 0.1 | 52 | 2 | 0.196 | 0.014 | 0.47 | 0.07 | quartz | 0.47 | 0.53 | 0.08 | 0.74 | 0.08 |
| | | | 0.25 | 0 | 3.08 | 0.85 | 0.15 | 1.15 | 0.1 | 52 | 2 | 0.196 | 0.014 | 0.05 | 0.02 | quartz | 0.05 | 0.06 | 0.02 | 0.28 | 0.01 |
| 28 | 0.27 | | 0.95 | 0.1 | | | | | | | | | | - | - | quartz | - | - | - | 1.04 | 0.11 |
| 2 | 0.30 | | 0.85 | 0.1 | | | | | | | | | | - | - | quartz | - | - | - | 0.93 | 0.10 |
| -1 | 0.27 | | 0.7 | 0.1 | | | | | | | | | | - | - | quartz | - | - | - | 0.76 | 0.10 |
| | | | 1.1 | 0.1 | | | | | | | | | | - | - | quartz | - | - | - | 1.20 | 0.07 |
| | | | 0.78 | 0 | | | | | | | | | | - | - | quartz | - | - | - | 0.85 | 0.04 |
| | | | 0.82 | 0 | | | | | | | | | | - | - | quartz | - | - | - | 0.89 | 0.04 |
| 230 | | | 44.3 | 4.8 | | | | | | | | | | - | - | tissue | - | - | - | 40.57 | 4.40 |
| 160 | | | 7.75 | 1 | 2.18 | 1.00 | 0.28 | 1.09 | 0.3 | 50 | 5 | 0.164 | 0.033 | 7.59 | 0.96 | tissue | 6.95 | 6.95 | 0.88 | 7.10 | 0.88 |
| | | | 1.16 | 0.2 | 1.82 | 1.00 | 0.22 | 1.05 | 0.06 | 60 | 3 | 0.172 | 0.019 | 0.99 | 0.24 | tissue | 0.90 | 0.90 | 0.22 | 1.06 | 0.22 |
| | | | 1.32 | 0.2 | 2.18 | 1.00 | 0.28 | 1.09 | 0.3 | 50 | 5 | 0.164 | 0.033 | 1.16 | 0.21 | tissue | 1.06 | 1.06 | 0.19 | 1.21 | 0.19 |
| | | | 1.3 | 0.2 | 2.18 | 1.00 | 0.28 | 1.09 | 0.3 | 50 | 5 | 0.164 | 0.033 | 1.14 | 0.22 | tissue | 1.04 | 1.04 | 0.20 | 1.19 | 0.20 |
| | | | 0.71 | 0.1 | 2.18 | 1.00 | 0.28 | 1.09 | 0.3 | 50 | 5 | 0.164 | 0.033 | 0.55 | 0.08 | tissue | 0.50 | 0.50 | 0.07 | 0.65 | 0.06 |
| | | | 0.45 | 0.1 | 2.95 | 1.00 | 0.38 | 1.1 | 0.04 | 80 | 15 | 0.324 | 0.069 | 0.13 | 0.10 | tissue | 0.12 | 0.12 | 0.09 | 0.41 | 0.06 |
| | | | 0.33 | 0 | 2.95 | 1.00 | 0.38 | 1.1 | 0.04 | 80 | 15 | 0.324 | 0.069 | 0.01 | 0.08 | tissue | 0.01 | 0.01 | 0.07 | 0.30 | 0.04 |
| | | | 0.27 | 0.1 | 2.95 | 1.00 | 0.38 | 1.1 | 0.04 | 80 | 15 | 0.324 | 0.069 | -0.05 | 0.09 | tissue | -0.05 | -0.05 | 0.08 | 0.25 | 0.05 |
| | | | 0.32 | 0.1 | 2.95 | 1.00 | 0.38 | 1.1 | 0.04 | 80 | 15 | 0.324 | 0.069 | 0.00 | 0.15 | tissue | 0.00 | 0.00 | 0.13 | 0.29 | 0.12 |
| | | | 0.24 | 0.1 | 2.95 | 1.00 | 0.38 | 1.1 | 0.04 | 80 | 15 | 0.324 | 0.069 | -0.08 | 0.11 | tissue | -0.08 | -0.08 | 0.10 | 0.22 | 0.07 |
| | | | 0.21 | 0.1 | 2.95 | 1.00 | 0.38 | 1.1 | 0.04 | 80 | 15 | 0.324 | 0.069 | -0.11 | 0.10 | tissue | -0.10 | -0.10 | 0.09 | 0.19 | 0.06 |
| | | | 0.21 | 0.2 | 2.62 | 1.00 | 0.47 | 1.11 | 0.05 | 60 | 12 | 0.224 | 0.055 | -0.01 | 0.16 | tissue | -0.01 | -0.01 | 0.15 | 0.19 | 0.14 |
| 43 | N | | 6.57 | 0 | | | | | | | | | | - | - | tissue | - | - | - | 5.90 | 0.01 |
| N | N | | 0.59 | 0.1 | | | | | | | | | | - | - | Roentgen | - | - | - | 0.50 | 0.11 |
| N | N | | 4.3 | 0.7 | | | | | | | | | | - | - | Roentgen | - | - | - | 3.67 | 0.60 |
| 0 | N | Y | 1.25 | 0 | | | | | | | | | | - | - | Roentgen | - | - | - | 1.07 | 0.01 |
| 0 | N | Y | 1.12 | 0 | | | | | | | | | | - | - | Roentgen | - | - | - | 0.95 | 0.01 |
| 0 | N | Y | 1.07 | 0 | | | | | | | | | | - | - | Roentgen | - | - | - | 0.91 | 0.01 |
| 21 | 0.84 | | 0.95 | 0.1 | | | | | | | | | | - | - | quartz | - | - | - | 1.01 | 0.11 |
| 20 | 0.81 | | 0.8 | 0.1 | | | | | | | | | | - | - | quartz | - | - | - | 0.85 | 0.10 |
| 26 | 1.00 | | 0.73 | 0.1 | | | | | | | | | | - | - | quartz | - | - | - | 0.77 | 0.08 |
| | | | 0.969 | 0 | | | | | | | | | | - | - | quartz | - | - | - | 1.08 | 0.05 |
| | | | 0.793 | 0 | | | | | | | | | | - | - | quartz | - | - | - | 0.88 | 0.02 |
| | | | 0.663 | 0 | | | | | | | | | | - | - | quartz | - | - | - | 0.74 | 0.02 |

samples from Hiroshima University and found them to be free of dose-dependent sensitivity changes to within 6 %.

**Pre-dose Thermoluminescence Dosimetry**

**Basic Procedures.** The pre-dose TL technique[13] is based upon the dose-dependent increase in sensitivity observed in the 110 °C TL peak of quartz. This peak is not normally seen in an old sample because it will have faded due to the shallow trap depth of the associated electrons. It can be seen by giving the sample a small test dose and then performing a glow curve run in which the sample is heated to about 150 °C. If the sample has received a prior dose of radiation and is heated to around 500 °C ("thermal activation"), subsequent excitation of the 110 °C peak with a test dose will reveal an increase in sensitivity of the peak. This increase is proportional to the dose accumulated ("pre-dose") prior to the thermal activation. The effect is depicted in Figure 12 where $S_o$ is the initial sensitivity of the sample measured with a small 1 rad test dose. $S_N$ is the sensitivity measured (again with a 1 rad test dose) after the sample has been heated to 500 °C. A calibrating dose followed by thermal activation produces yet another increase in sensitivity ($S_{N+\beta}$).

Accrued dose is estimated with a single portion of sample by taking the ratio of the sensitivity change due to the accrued dose to the calibrating dose and multiplying by the

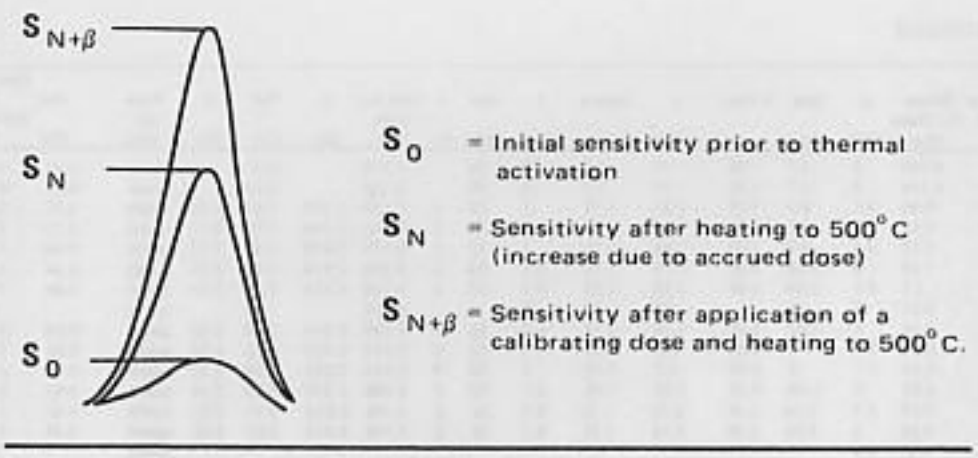


*Table 12. Sensitivity increase of 110°C thermoluminescence peak of quartz.*

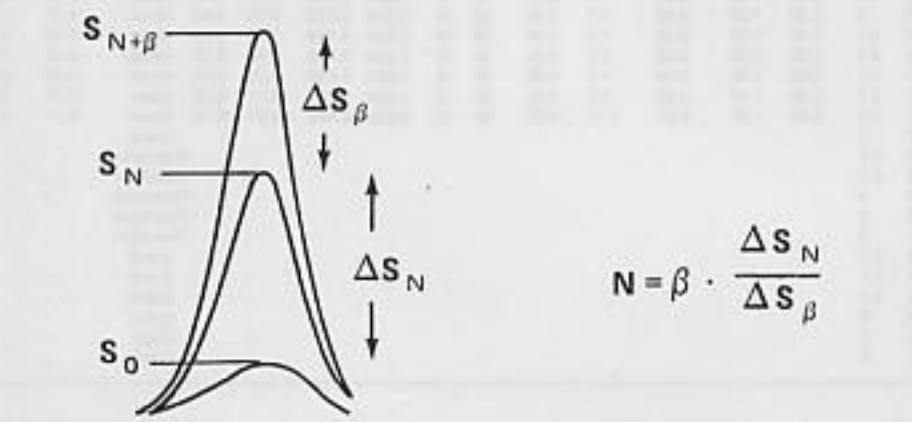


*Figure 13. Basic dose estimation with the pre-dose technique (single sample).*

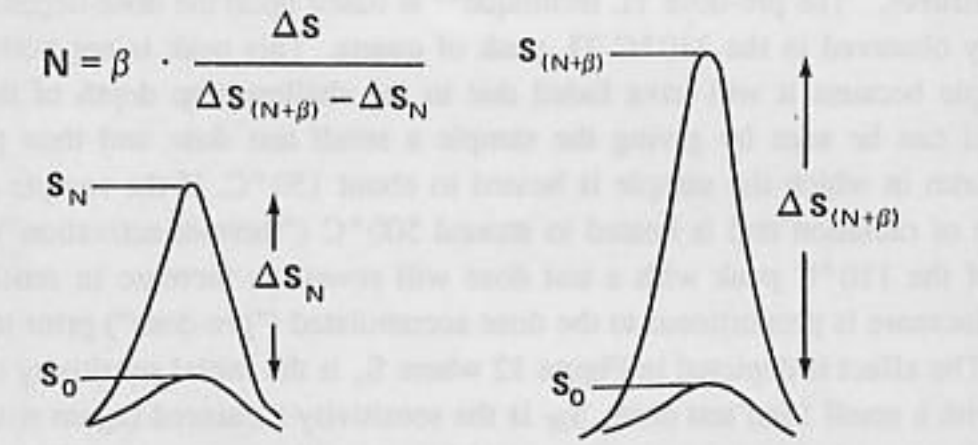


*Figure 14. Basic dose estimation with the pre-dose technique (multiple samples).*

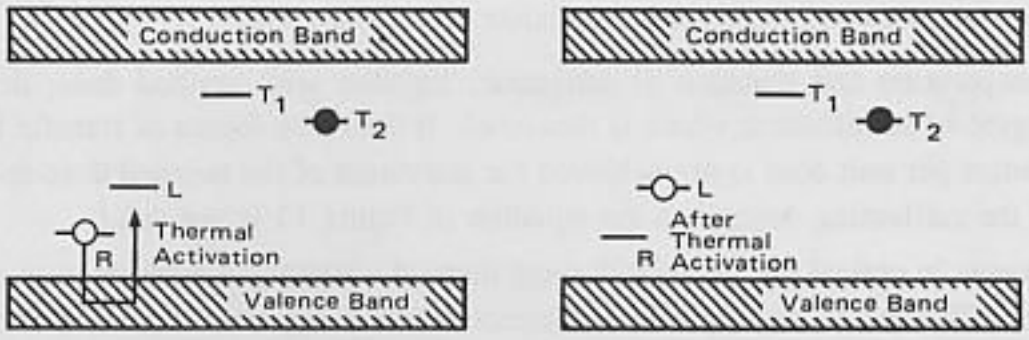


In this model holes are selectively trapped at R traps during irradiation, while electrons are trapped at $T_1$ (and $T_2$, included to maintain charge balance). Thermal activation to temperatures in excess of 500°C causes transfer of holes from R traps to luminescence centers (L) thereby activating them. The postulated "deactivated" state of L centers is thus shown as L centers that are neutral (i.e., have not captured holes), the increase in sensitivity is due to the increase in the population of active L centers. Because of the short half-life of electrons in $T_1$, these traps are shown without associated electrons.

*Figure 15. The Zimmerman model for pre-dose sensitization.*

calibrating dose $\beta$ (the multiple activation procedure, Figure 13). A similar procedure is used for dose estimation using two aliquots of sample with the exception that prior to thermal activation one sample is given a calibrating dose of radiation additional to the accrued dose (the additive dose procedure Figure 14).

**The Pre-dose Model.** The model proposed for the pre-dose phenomenon[21] assumes that there are two states for luminescence centers, an "activated" state in which the center is capable of receiving an electron with the emission of light and a "deactivated" state in which the center cannot receive an electron. A deactivated center can be activated by receiving a hole, and an activated center can be deactivated by losing a hole. The model, described in Figure 15, includes electron traps $T_1$ and $T_2$, hole traps L (the luminescence centers), and R (the reservoir centers). During exposure to radiation, because of their presumed larger capture cross section, reservoir centers R capture hole preferentially to luminescence centers L, and electron traps $T_1$ and $T_2$ capture electrons. The depth of $T_1$ is sufficiently small that the electrons remain with a half-life of only hours whereas the electrons in $T_2$ remain trapped indefinitely. The holes trapped in R are very stable at room temperature, but are dislodged at high temperature. Once they are dislodged during thermal treatment, the holes become trapped at L. Those that do recombine with R are immediately rejected. In this process luminescence centers L become activated and are then capable of electron capture and photon emission. The net result of this procedure is that the population of L centers has increased over that initially present and the probability is increased that any future electron ejected from $T_1$ will be captured at L with the emission of light. It is this increase in the population of L centers that results in the observed increase in the sensitivity of the 110°C TL peak of quartz.

**Variations of the Pre-dose Technique.** For the equation in Figure 13 to be valid the sensitization per unit dose induced by the calibrating dose must be equal to that of the dose

being measured. Several factors can invalidate this assumption:

1. Temperature and duration of activation, together with applied dose, determine the degree of sensitization which is measured. If the same degree of transfer from R to L centers per unit dose is not achieved for activation of the accrued dose and activation of the calibrating dose, then the equation of Figure 13 is not valid.
2. Change in optical properties following thermal activation are common in certain samples. Changes in degree of transmittance result in apparent increases or decreases in the degree of sensitization per unit dose of radiation for the calibrating dose relative to that for the accrued dose.
3. Saturation effects are seen with the pre-dose TL technique at doses in excess of several 100 rad, considerably below dose levels of nonlinearity with high temperature techniques.
4. Changes in the population of R traps following thermal activation have been suggested as another factor influencing the dose/sensitization ratio.[19]
5. Thermal quenching or deactivation of L centers during heating could effect the measurement of sensitization change if not accounted for.
6. This is also true of radiation quenching, the decrease in sensitivity seen following application of a large calibrating dose.

These factors potentially affect the degree of sensitization observed as a function of dose and complicate pre-dose analysis. Numerous modifications and additions to the original methods of analysis have resulted.

*Thermal Activation Characteristic.* A plot of sensitivity of a pre-dose sample as a function of activation temperature is shown in Figure 16. This thermal activation characteristic (TAC) is performed prior to any dose estimation procedure to identify the temperature of maximum sensitization. A second TAC to examine the activation of the calibrating dose is also performed, Figure 17. Since the degree of activation is a function of time as well as temperature, the shape of the TAC will be shifted to lower temperatures for samples heated at lower heating rates or samples held at the activation temperature for longer periods of time. Occasionally, even when heating rates and hold times are identical, the two curves of the TAC will show a shift in maximum temperature. This shift, if not accounted for by corresponding changes in applied temperature during analysis, may result in different degrees of activation of the calibrating dose relative to that for the accrued dose, thus introducing a bias into the final estimate.

*The Radiation Quenching Correction.* The radiation quenching correction (Figure 18)[22,23] was a modification proposed to account for sublinear growth of sensitivity. The effect was attributed to L center deactivation resulting from application of the calibrating dose. The correction involves measurement of the sensitivity of the sample following application of the calibrating dose but prior to thermal activation. This sensitivity level $S_N$ is taken as the new baseline against which the subsequent increase in sensitivity is measured.

*Additive Dose Pre-dose Analysis.* Since the heating and cooling rate in the kiln differ drastically from those on the TL reader heating plate, it is not surprising to find occasional changes in sample properties following the first laboratory heating and cooling. The new

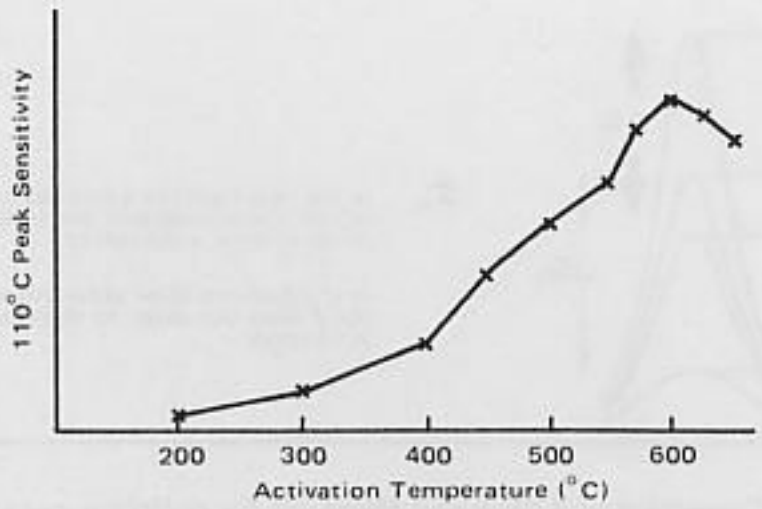


The sensitivity of a pre-dosed sample is gradually increased by successive heatings to higher temperatures. The sensitivity is measured after each heating. Temperatures for maximum sensitization rarely occur as low as 500°C in modern bricks and tiles.

*Figure 16. Thermal activation characteristic.*

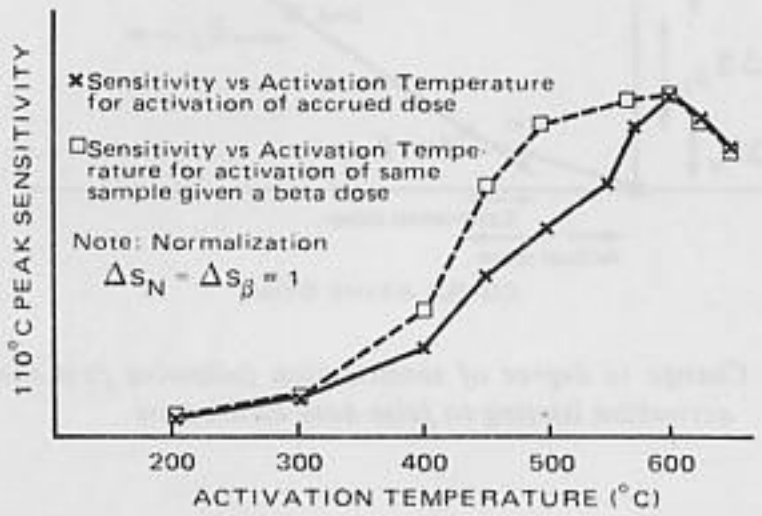


Such differences in TAC's can indicate possible ambient activation or change in sensitization following 1st set of activations.

*Figure 17. Diagnostic thermal activation characteristic.*

properties may then remain stable for subsequent laboratory heatings, complicating detection of the change.

The additive dose pre-dose method, initially proposed by Fleming, will, under ideal conditions, detect changes in degree of sensitization. The method is similar in many respects to the additive dose procedure of high temperature analysis[13] but in practice it suffers some serious shortcomings. The method involves measuring the sensitivity increase due to the accrued dose on one portion of the sample and comparing this to the increase in sensitivity due to the accrued dose plus a calibrating dose applied to a second portion of the sample.

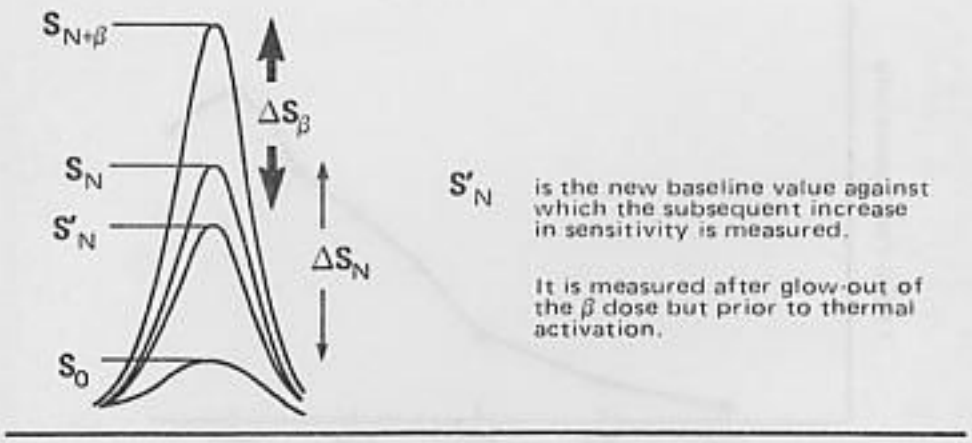


*Figure 18. Correction of Aitken and Murray[22] for radiation quenching.*

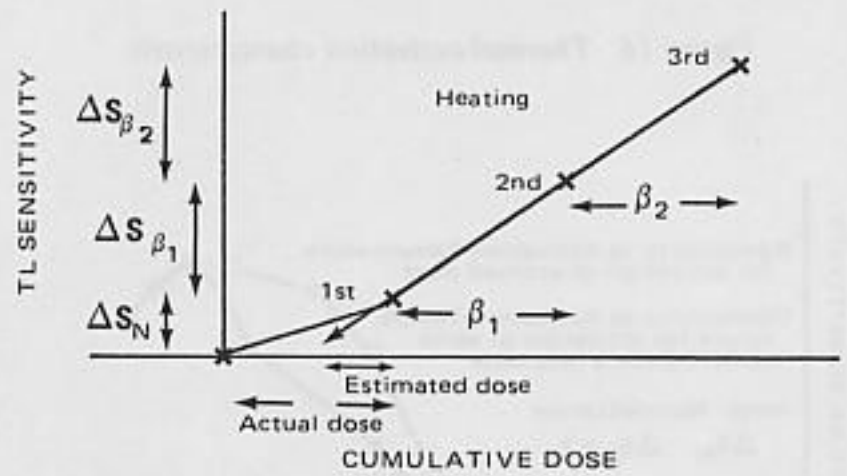


*Figure 19. Change in degree of sensitization following first thermal activation leading to false dose estimation.*

By normalizing to weight, or initial sensitivity, an estimate of accrued dose unaffected by thermal stress may be obtained (Figure 14):

$$D_N = (\Delta S_N / (\Delta S_{N+\beta} - \Delta S_N))\,\beta \tag{7}$$

Inconsistencies and problems with normalization unfortunately render this method the least precise of the pre-dose methods.

*The Spiking Method.* The spiking method of pre-dose analysis[8] as initially described was a diagnostic test designed as a qualitative check on sensitization change following thermal activation (Figure 19).[19] The procedure involved application of an additive dose (or spike) on top of the accrued dose prior to analysis. By proceeding with the normal multiple activation analysis (Figure 13) following spiking and subtracting out the spike dose from the total dose estimate, a measure of accrued dose was obtained. If this value was not significantly different from the accrued dose estimate obtained by the nonspiked multiple activation analysis, then

$$D(1) = \beta \frac{\Delta S_N}{\Delta S_\beta}$$ Estimate of accrued dose only

$$D(2) = \left( \beta \frac{\Delta S_{(N+\beta_0)}}{\Delta S_\beta} \right)$$ Estimate of accrued dose plus the dose added prior to analysis ($\beta_0$)

$$D(\text{actual}) = \frac{D(1) \cdot \beta_0}{D(2) - D(1)}$$ Evaluation of Accrued Dose

*Figure 20. Spiking method.*

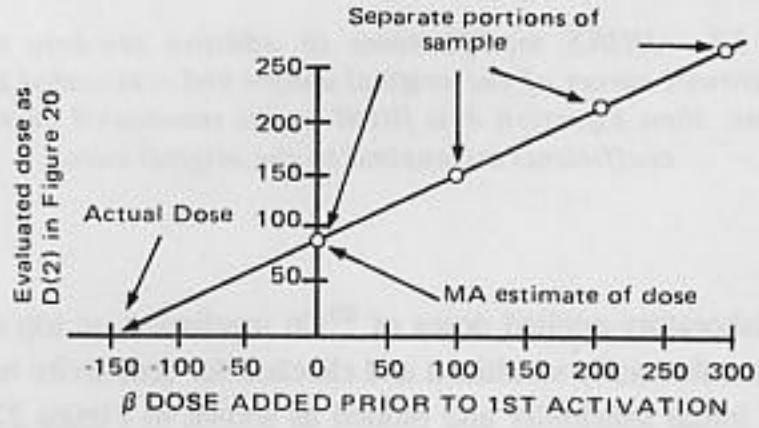


*Figure 21. Modified additive dose procedure.*

no change in sensitization was thought to have occurred. If a lower dose was obtained with the spiking method then a change in sensitization following the first activation had occurred and the actual accrued dose was higher than that measured with the multiple activation procedure. The sample was therefore excluded from further analysis. The spiking method was later modified to enable actual estimates of the accrued dose to be obtained (Figure 20).[24]

*Modified Additive Dose Pre-dose Procedure.* The modified additive dose pre-dose procedure (Figure 21)[20,24] is similar in principle and sample analysis to the spike procedure but offers a graphical method of data reduction. A plot is made of estimated dose obtained from pre-dosed samples versus the amount of laboratory pre-dose. Extrapolating through the data points back to the applied dose axis provides an estimate of accrued dose independent of sensitivity change. The intercept on the measured dose axis should correspond to the dose estimate obtained with the multiple activation method alone.

*JNIRS Modifications to the Additive Dose Procedure.* Saturation effects encountered with the pre-dose technique were described by Chen,[25] and a method for overcoming nonlinearity of growth of sensitivity was described. The additive dose pre-dose technique employed at JNIRS (Appendix 4-1) incorporates aspects of this approach. The method used at JNIRS involves initial analysis using the additive dose pre-dose procedures. Multiple aliquots of the

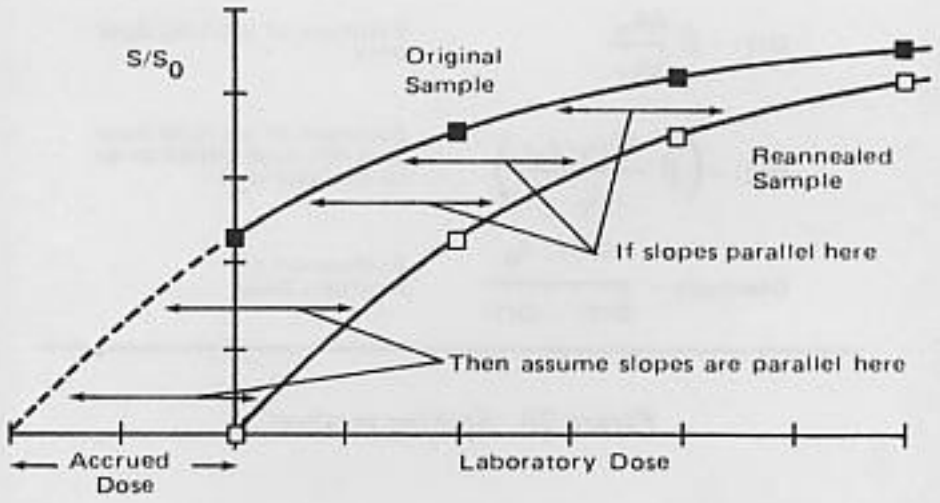


*Figure 22. JNIRS modifications to additive pre-dose technique. If the growth curves of the original sample and reannealed sample are the same, then Equation 8 is fitted to the reannealed curve and the coefficients are applied to the original curve.*

sample are given laboratory-applied doses of $^{60}Co$ irradiation on top of the accrued doses. The samples are then thermally sensitized and checked for sensitivity increase. These values are normalized by initial sensitivity and plotted as shown in Figure 22. A least squares fit is then made of the data using the following equation:

$$R = R_{\infty}(1 - e^{-\lambda D}) \tag{8}$$

where $R_{\infty}$ is the maximum level of sensitivity attained at full L center saturation, R is the sensitivity of the sample at any intermediate level determined by the additive dose, D, and $\lambda$ is a constant. By extrapolating to 0 on the dose axis an estimate of the accrued dose value, unbiased by saturation effects, should be obtained.

The JNIRS group carried the method one step further by annealing the measured samples back to their original levels of sensitivity, redosing these annealed samples and repeating the measurements. In this way the growth of sensitivity at doses lower than the accrued dose may be examined; and, assuming that the reannealed growth characteristic faithfully replicates the original, dose estimates may be made from a comparison of the two curves.

## MEASUREMENT OF BACKGROUND RADIATION DOSE

### Dose Contribution from Natural Radiation

Thermoluminescence dating techniques are based on the assumption that a dose due to natural radiation will be deposited in a sample uniformly with time. Since the age of the sample is determined directly from the measurement of total dose to the sample (determined by TL techniques) and measurements of the rate at which various contributors to dose (alpha, beta, gamma, and cosmic radiation) accumulate with time, uncertainties in the measurement

of background dose rate translate directly to errors in the estimate of sample age. For this reason a great deal of effort has gone into investigating the various parameters and errors associated with measurement of dose rate in archaeological samples.[11]

For A-bomb exposed samples the errors associated with measurements of background radiation are of less concern for high A-bomb doses, and of greater concern for low A-bomb doses. For a sample with an A-bomb dose of 80 rad and a background dose of 20 rad, a 20% error in measurement of background dose will result in a 5% error in estimation of A-bomb dose. For a sample with an A-bomb dose of 4 rad and with background dose and error as above, the error in the estimate of A-bomb dose increases to 100%. The errors shown in Table 2 reflect the error contributions for measurement of natural background radiation.

The major contributors of background dose include radionuclides in and around the samples, primarily the $^{235}U$, $^{238}U$, and $^{232}Th$ series and $^{40}K$ and $^{87}Rb$ (Table 3) plus cosmic rays. Dose rates for the alpha, beta, gamma, and cosmic radiation must be included or excluded depending upon the TL technique employed. The alpha-particle component is not considered with the high temperature (i.e., quartz inclusion) technique because of the sample etching treatment; and the effectiveness of alpha particles in inducing pre-dose sensitization has been shown to be negligible.[26]

## Measurement of Background Dose-rate

Many methods are available for determining natural background dose-rates. They include alpha-particle counting, flame photometry, beta-particle TL, fission track analysis, neutron activation analysis, autoradiography, gamma-ray spectrometry, alpha-particle spectrometry, and gamma-ray TL. The techniques used in this study include beta-particle TL (DUR, JNIRS, NUE, UU) and alpha-particle counting (OXF) for determining the beta-particle contribution, and gamma-ray TL for determining the gamma- and cosmic-ray contribution to background.

**Sources of Error in Background Measurements.** An implicit assumption in the measurement of background dose-rate is that the value measured following sample collection is the same as that experienced over the lifetime of the sample. Several factors can invalidate this assumption.

*Disequilibrium Caused by Firing of the Sample.* It is possible that the intense temperatures of firing (1100 to 1200 °C) could volatilize and drive off certain daughter products such as radium with its 1140 °C boiling point. If this did occur then the dose-rate to a sample from the thorium series ($^{228}Ra$, 6.7-year half-life) would increase gradually over the 40-year post-firing lifetime of the sample. The same would hold for the $^{235}U$ series ($^{223}Ra$, 11.4-day half-life), however the $^{223}Ra$ would grow back so rapidly that the effect of the transient disequilibrium would not be significant. After firing, the $^{238}U$ series ($^{226}Ra$, 1600-year half-life) would not suffer further changes in dose-rate since significant ingrowth of $^{226}Ra$ would not occur over a 40-year period.* Tests were not made for firing-induced chain disequilibrium in the Hiroshima and Nagasaki samples.

*Radon Emanation.* $^{222}Rn$ with a 3.82-day half-life can diffuse through the porous structure of some ceramics. In addition, the form of the sample during background measurement may

*Errors in beta-particle dose-rate determinations would occur with alpha-particle counting techniques since chain equlibrium is assumed in those calculations.

Thorium-232 Series

| Nuclide | Half-life | B.P. |
|---|---|---|
| Thorium-232 | $14.0 \times 10^9$ yr | 4790°C |
| ↓α | | |
| Radium-228 | 5.8 yr | 1140 |
| ↓α | | |
| Actinium-228 | 6.13 yr | 3200 |
| ↓α | | |
| Thorium-228 | 1.91 yr | 4790 |
| ↓α | | |
| Radium-224 | 3.7 d | 1140 |
| ↓α | | |
| Radon-220 | 56 sec | −62 |
| ↓α | | |
| Polonium-216 | 0.15 sec | 962 |
| ↓α | | |
| Lead-212 | 10.64 hr | 1740 |
| ↓α | | |
| Bismuth-212 | 1.01 hr | 1560 |
| ↓β (64%) ↓α (36%) | | |
| ↓ Tellurium-208 | 3.05 min | 990 |
| ↓ ↓β | | |
| Polonium-212 ↓ | $3.0 \times 10^{-7}$ sec | 962 |
| ↓α ↓ | | |
| Lead-208 | Stable | 1740 |

Uranium-235 Series

| Nuclide | Half-life | B.P. |
|---|---|---|
| Uranium-235 | $0.704 \times 10^9$ yr | 3818°C |
| ↓α | | |
| Thorium-231 | 25.2 hr | 4790 |
| ↓β | | |
| Protectinium-231 | $32.7 \times 10^3$ yr | Very high |
| ↓α | | |
| Actinium-227 | 21.77 yr | 3200 |
| ↓β | | |
| Thorium-227 | 18.72 d | 4790 |
| ↓α | | |
| Radium-223 | 11.4 d | 1140 |
| ↓α | | |
| Radon-219 | 4.0 sec | −62 |
| ↓α | | |
| Polonium-215 | $1.8 \times 10^{-3}$ sec | 962 |
| ↓α | | |
| Lead-211 | 36.1 min | 1740 |
| ↓β | | |
| Bismuth-211 | 2.14 min | 1560 |
| ↓α | | |
| Tellurium-207 | 4.77 min | 990 |
| ↓β | | |
| Lead-207 | Stable | 1740 |

Uranium-238 Series

| Nuclide | Half-life | B.P. |
|---|---|---|
| Uranium-238 | $4.46 \times 10^9$ yr | 3818°C |
| ↓α | | |
| Thorium-234 | 24.1 d | 4790 |
| ↓β | | |
| Protectinium-234 | 1.17 min | Very high |
| ↓β | | |
| Uranium-234 | $245 \times 10^3$ yr | 3818 |
| ↓α | | |
| Thorium-230 | $75 \times 10^3$ yr | 4790 |
| ↓α | | |
| Radium-226 | 1600 yr | 1140 |
| ↓α | | |
| Radon-222 | 3.82 d | −62 |
| ↓α | | |
| Polonium-218 | 3.11 min | 962 |
| ↓α | | |
| Lead-214 | 26.8 min | 1740 |
| ↓β | | |
| Bismuth-214 | 19.9 min | 1560 |
| ↓β | | |
| Polonium-214 | $1.63 \times 10^{-4}$ sec | 962 |
| ↓α | | |
| Lead-210 | 22.3 yr | 1740 |
| ↓β | | |
| Bismuth-210 | 5.01 d | 1560 |
| ↓β | | |
| Polonium-210 | 138 d | 962 |
| ↓α | | |
| Lead-206 | Stable | 1740 |

**Table 3. Natural Radioactive Decay Series.**

be such as to allow more (powdered sample) or less (sealed sample) escape of radon than was experienced in situ. This is particularly a problem with background measurements made using alpha-particle counting techniques, but it could also be significant with beta-particle TL depending upon the length of time the sample had been stored prior to measurement.

*Attenuation by Measuring Device.* If measurement is made using beta-particle TL, shielding must be included to absorb alpha particles. Unfortunately the alpha-particle shielding will also absorb low energy beta particles necessitating inclusion of an attenuation correction in calibration of beta-particle TL units. The same occurs with gamma-ray TL measurements where correction must be made for attenuation of gamma rays by the beta-particle absorbing dosimeter capsule.

*Matrix Corrections.* Differences in electron stopping power or gamma-ray attenuation between the walls of the measuring capsule and the dosimeter used or the quartz grains, can result in edge effects which add to the error associated with the calculation of dose delivered to the quartz grains. Use of a quartz-equivalent phosphor, such as $Mg_2SiO_4$ or $Al_2O_3$ in a low-activity glass or quartz capsule, will avoid such problems regardless of U, Th, and K ratios. Calibration of a nonquartz-equivalent dosimeter and capsule in doped standard blocks will also reduce uncertainty.

*Homogeneity of Radiation Field.* Crystals irradiated within a brick or tile sample will experience essentially homogeneous exposure from beta particles if they are located deeper than 2 mm from the edge of the sample. Crystals in the outer 2 mm will experience lower doses of beta radiation and are routinely excluded from analysis.

The same is true, but to a lesser extent, for the measurement of gamma rays using in situ gamma-ray TL methods. A detector, placed on the outside of a wall being measured, will detect a smaller contribution of the gamma rays which originate from within the sample than it would if the detector were implanted within the matrix. Unfortunately, the thickness of the tiles used in this study precluded the implantation of TL dosimeters. The associated errors have not yet been fully investigated.

*Variation in Decay Series Ratios.* Beta-particle TL measurements in the laboratory also include a component of dose from gamma rays emitted from the sample. Since the ratio of infinite matrix gamma-ray dose to beta-particle dose varies from 0.3 for K, 0.8 for U, to 1.8 for Th,[11] a sample with a high K to Th ratio will experience a much lower gamma-ray component than will a sample with ratios reversed. Furthermore, the quantity of sample used for measurement is important since large samples will contribute a higher gamma-ray dose than will smaller samples (the beta-particle component will of course remain constant once the maximum beta-particle range of several millimeters has been reached).

*Beta-particle Attenuation by Quartz Grains.* All of the methods for beta-particle TL calibration are either specific for measurement of crystals of a particular size or apply attenuation factors to measured values depending on the size of the grains actually measured. A complication arises if grains are found in clumps or agglomerations inside the brick or tile,[27] because agglomerations of grains will increase the beta-particle attenuation experienced by the individual grains as indicated in Figure 23. Micrographs of brick and tile sections are shown in Figures 24 and 25.

The most effective way to avoid problems associated with most of the items above is through the use of adequate calibration programs. For beta-particle dosimetry, a program with separate standards for U, Th, and $^{40}K$ should be used, and for gamma-ray dosimetry, a program with separate standards for assessing attenuation and the effects of different stopping powers should be used.

**Methods of Calibration of Beta-particle TL Units.** Two methods of calibration for beta-particle TL units were used by the laboratories. With the first calibration method U, Th, and K standards of known activity were measured. The beta-particle component of dose-rate to a hypothetical point absorber in a beta particle thick (infinite-matrix) standards matrix is also calculated. The TL values measured are compared to the calculated infinite-matrix point-absorber values and a calibration factor is obtained. An advantage of this method is

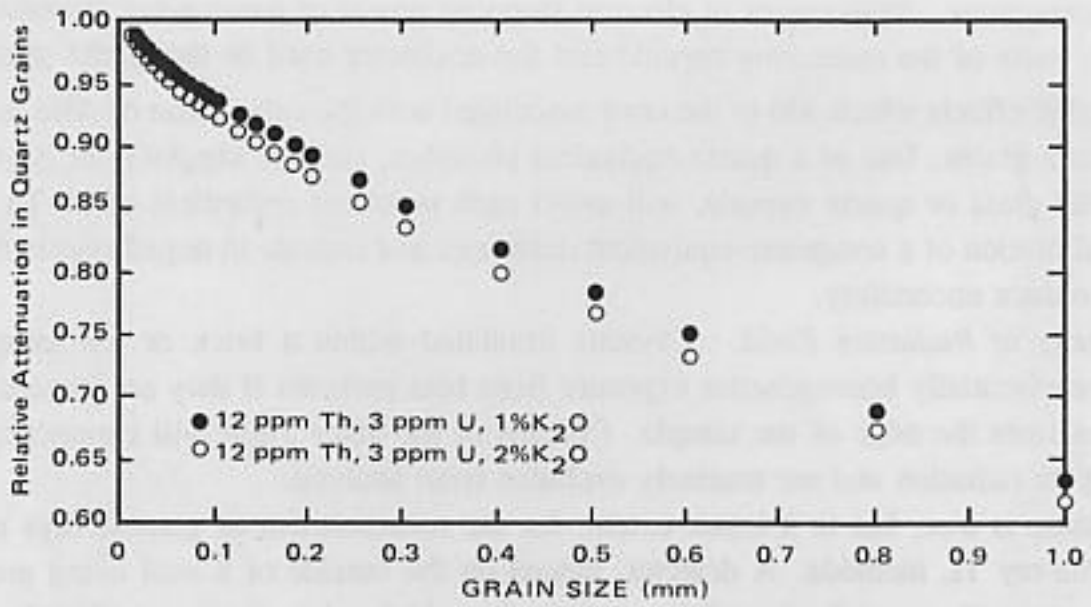


*Figure 23. Relative attenuation fractions in quartz grains for two concentrations of radionuclides (Mejdahl, 1979).*

that the component of dose due to sample gamma rays is excluded. Since values obtained are for infinitely small quartz grains, a grain-size dependent beta-particle attenuation factor (Figure 23) must be applied to the measured values.

The second calibration method involves sandwiching grains of phosphor of the same size as would be used for high temperature or pre-dose analysis between two layers of sample, but separated from them by an alpha particle thick absorber . In this manner $4\pi$ geometry is approximated. Measurements are also made of beta-particle attenuation due to the alpha-particle absorber (by measuring various thicknesses), and the dose rate measured by the phosphor is increased by this amount. Actual calibration of this method is by irradiation of the phosphor with a previously calibrated $^{60}Co$ source. Measurements of background dose to the Hiroshima and Nagasaki samples were performed by a variety of techniques in various laboratories.

*Beta-particle TL (DUR and UU).* The beta-particle TL apparatus used at DUR and UU were identical (the UU system was constructed by the Durham laboratory). The apparatus[18] consists of a Perspex sample container with an inside diameter of 15 mm in which approximately 1.5 g of crushed material is placed to a depth of 6 mm. The sample rests directly on an alpha-particle absorbing Melinex (Mylar) window (17.5 mg/cm$^2$) and a dosimeter of natural $CaF_2$ sits directly under the Melinex window and absorbs beta particles from the sample over the period of exposure (7 to 14 days). The units, housed in lead containers, were calibrated by exposing the dosimeters to standard U and Th sands and KCl (method 1). Background gamma radiation was measured using high purity quartz in the sample container and subtracting the resulting environmental contribution from the total.

*Beta-particle TL (NUE).* Beta-particle TL measurements at NUE involved compression of grains <75 $\mu$m in diameter into two circular plates of 45 mm diameter and a thickness of 3 mm (Appendix 4-2). Approximately 60 mg of $CaSO_4$ : Tm grains of 105 to 149 $\mu$m diameter were then spread in a monolayer between the two plates. The grains were separated from

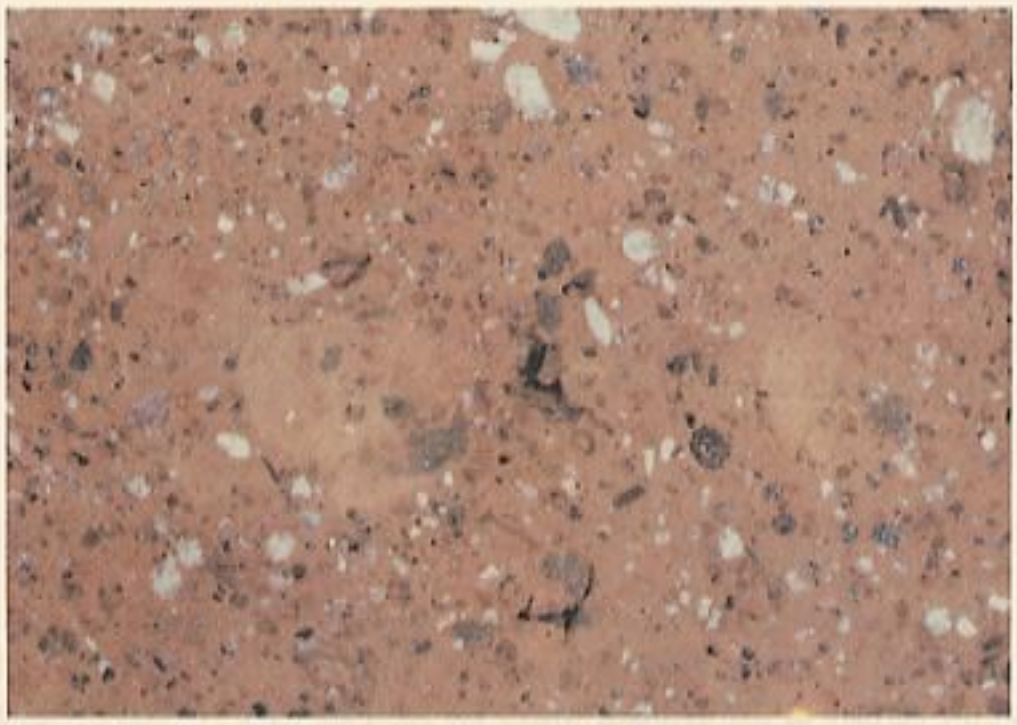

*Figure 24. Micrograph (×3) of Nagasaki Ieno-cho brick sample NAIE08.*

*Figure 25. Micrograph (×3) of Hiroshima University tile sample UHFS03.*

the sample by polyethylene sheets (40 $\mu$m, 3.5 mg/cm$^2$ thickness) and stored for two weeks in a lead container. Beta-particle attenuation due to the thickness of the polyethylene sheet was measured using JG-1 standard sands[28] and external background gamma radiation was measured and subtracted from the total.

*Beta-particle TL (JNIRS).* The background dose for beta particles coming from natural radionuclides in brick and tile specimens was measured with an experimental arrangement specified in Appendix 4-1. For the measurement of beta particles, $Mg_2SiO_4$ (MSO) TL powder (Kasei Optonics Ltd, Tokyo) was used with a grain size of about 100 to 150 $\mu$m diameter. A polyethylene film 100 $\mu$m in thickness was used to absorb the alpha particles. The external gamma-ray background was measured for environmental radiation using a lucite absorber 1.5 cm thick to stop beta particles from reaching the MSO placed on top of it. Each of the cells was left in a lead shielded container of 15 cm thickness for a period of six months. A correction factor of 0.7 for the absorption of beta particles in the polyethylene film was used.

**Gamma-ray Background Measurements.** Gamma-ray background measurements were carried out by NUE and JNIRS.

*NUE Gamma-ray Measurements.* $CaSO_4$ : Tm crystals were contained in 1 mm thick polyethylene capsules placed in copper tubes with a 1 mm thick wall. Samples were left for about 100 days on the surface of the building where the samples were collected (Appendix 4-2).

*JNIRS Gamma-ray Measurements.* The background gamma-ray dose from environmental radiation and from wall material was determined using MSO TL detectors placed at various depths in an aluminium plate 1 cm thick. Each dosimeter cell was left for six months on the surface of the building from which the sample was taken (Appendix 4-1).

## RESULTS AND DISCUSSION

### Environmental, A-bomb, and Preparation Effects

Many of the TL procedures described above address problems inherent with TL analysis of naturally occurring phosphors. These tests were applied to many of the Hiroshima and Nagasaki samples (Table 2). Additional tests were made to verify that other factors were not biasing dose estimates.

Most of the analyzed tile samples were removed from structures that had not been damaged by fire. Independent checks for heating effects on TL properties were made using two TL techniques: (1) the plateau test for high temperature analysis, which would reveal instances of partial TL annealing*, and (2) ultraviolet reversal of sensitivity for pre-dose analyzed samples. Samples which revealed heating effects were excluded from further analysis.

The possible addition of spurious components or reduction of TL signal as a result of sample crushing was examined by JNIRS (Appendix 4-1) for the high temperature technique and pre-dose technique and by UU (Appendix 4-6) for the pre-dose technique. No effects were seen within the limits of error for the two tests.

Most laboratories obtained quartz grains from bricks and tiles by an initial magnetic separation of the crushed and sieved sample grains. Several laboratories subjected this material to additional purification by treatment in hydrofluoric acid. The acid treatment varied from one hour in concentrated hydrogen fluoride (HF) to several minutes wash in

*Complete reannealing would not be detected by the plateau test; however, other factors, including surface changes and dose estimates equal to natural background levels, would be present.

dilute HF. Results from etched and unetched Ieno-cho wall brick samples indicated that the HF washing procedure was producing dose estimates that were low compared to the fully etched or the untreated samples. This effect was substantiated in results of a more complete study of Ieno-cho wall samples analyzed by UU.

In a follow-up study of etching effects, nonmagnetic Ieno-cho wall crystals were treated in HF for varying times and at varying concentrations prior to TL analysis. Dose estimates from the fully etched samples (1 hr, 48 % HF) showed good precision of measurement ($\sigma < 5\%$) and a linear decrease in dose with increasing depth through the brick. The unetched samples showed greater variability in measurement; however, the mean for the entire brick (all three depths analyzed) did not differ significantly from the mean for the fully etched samples. Samples treated for three minutes in dilute HF, on the other hand, showed good precision ($\sigma < 8\%$) but significantly lower dose estimates (approximately 15 %) relative to the fully etched and unetched samples. X-ray diffraction analysis at DUR revealed that the sample contained a high percentage of Na feldspar (Appendix 4-7). Further tests on A-bomb exposed samples are underway.

The effect of fast neutrons on conventional TL properties of quartz was found to be negligible,[8] however, at high neutron doses small changes were seen in the thermal activation characteristics of pre-dose analyzed samples. Given the low doses from fast neutrons which would have occurred at 1400 m, any effects on the samples would appear to be small.

The increased energy absorption of quartz versus tissue at low gamma-ray energies (Figure 4) necessitates confirmation that significant doses of low energy gamma radiation were not present in the prompt or delayed gamma-ray spectra. Results in Chapter 3 confirm that doses from low-energy gamma rays (< 100 keV) were negligible relative to those from gamma rays with energies in excess of 1 MeV.

A comparison of dose estimates obtained with the pre-dose technique versus those obtained in the same laboratory with the high temperature technique (Appendix 4-4) suggests that a systematic error may exist between the two (pre-dose : high-temperature = $1.10 \pm 0.06$). Results from other laboratories do not reveal this bias when comparison is made between pre-dose and high temperature results on the same samples. Intercomparison samples were measured at DUR with both techniques and no significant differences were found (Appendix 4-7). A comparison of results obtained by UU using the pre-dose technique with high temperature results on the same samples by DUR and OXF also do not show higher values for the pre-dose technique (Table 4). The results of the US National Bureau of Standards (NBS) irradiated sample analyzed with the pre-dose technique at JNIRS, UU, and DUR also were not systematically higher than either the actual applied doses, or the values obtained with the high temperature technique at NUE.

**Interlaboratory Agreement**

The main objective of the TL studies is to provide measurements of A-bomb gamma-ray doses which may be compared with estimates derived from theoretical calculations.

The quantity measured by TL analysis is the dose to quartz grains of a specific size embedded in a matrix of variable composition whose original location is a specified distance from the front and rear surface of the brick or tile being examined. The brick or tile itself is uniquely oriented with respect to the blast and nearby walls, floors, pillars, etc., which

**Table 4. Hiroshima University Floor Tile Intercomparison.**

| Lab. | Place and Sample | Sample I.D. # | Sample Type | Distance (meters) | Grains µm | *TL Method | Gross (Gy) Unadjusted | Gross (Gy) Adjusted** | | Averages (Gy) Unadjusted | Averages (Gy) Adjusted** |
|---|---|---|---|---|---|---|---|---|---|---|---|
| N.U.E. | H.U.F.S. (Hiro. Univ.) | 4 | TILE | | 50-74 | HT | 0.69 | 0.67 | N.U.E. | 0.84 ± 0.09 | 0.82 ± 0.09 |
| N.U.E. | H.U.F.S. (Hiro. Univ.) | H-10-1 | TILE | | 50-74 | HT | 0.93 | 0.91 | | | |
| N.U.E. | H.U.F.S. (Hiro. Univ.) | H-10-2 | TILE | | 50-74 | HT | 0.88 | 0.86 | | | |
| N.U.E. | H.U.F.S. (Hiro. Univ.) | H-10-3 | TILE | | 50-74 | HT | 0.82 | 0.80 | | | |
| N.U.E. | H.U.F.S. (Hiro. Univ.) | H-10-4 | TILE | | 50-74 | HT | 0.88 | 0.86 | | | |
| DUR | H.U.F.S. (Hiro. Univ.) | UHFSFT02 | TILE | | 90-150 | HT | 0.77 | 0.84 | DUR | 0.78 ± 0.01 | 0.84 ± 0.01 |
| DUR | H.U.F.S. (Hiro. Univ.) | UHFSFT02 | TILE | | 90-150 | PD MAD | 0.78 | 0.85 | | | |
| OXF H | H.U.F.S. (Hiro. Univ.) | UHFSFT03 | TILE | | 90-125 | HT | 0.84 | 0.89 | Oxf H*** | 0.84 | 0.89 |
| OXF S | H.U.F.S. (Hiro. Univ.) | UHFSFT03 | TILE | | Slice | HT | 0.87 | 0.92 | | | |
| OXF S | H.U.F.S. (Hiro. Univ.) | UHFSFT03 | TILE | | Slice | PD-MA | 0.87 | 0.92 | | | |
| U.OF U. | H.U.F.S. (Hiro. Univ.) | UHFSFT02 | TILE | | 150-250 | PD-MA | 0.78 | 0.87 | UU | 0.76 ± 0.03 | 0.84 ± 0.03 |
| U.OF U. | H.U.F.S. (Hiro. Univ.) | UHFSFT03 | TILE | | 150-250 | PD-MA | 0.74 | 0.82 | | | |

*HT = High Temperature
PD = Pre-dose
MA = Pre-dose Multiple Activation
MAD = Pre-dose Modified Additive Dose

** Correction factors based on intercalibration using NBS irradiated MSO
DUR 1.09
JNIRS 1.00
NUE 0.98
OXF 1.06
U of U 1.11

*** Oxf Slices excluded due to uncertainty in background contribution

| | | |
|---|---|---|
| Mean (Gy) | 0.80 | 0.85 |
| Stdev (Gy) | 0.04 | 0.03 |
| Stdev (%) | 5.2% | 3.4% |

provide both shielding and scatter from neutrons and secondary gamma rays.

Thus, for a given free-field kerma at a specified distance from the hypocenter, the doses absorbed by individual grains in separate samples will differ. To accurately compare TL measurements of dose with the computational model, the significant parameters for each sample must be individually specified.

In making the comparison, a variation of the computer model applied to survivors is applied to the TL samples. The result is an estimate of dose to quartz grains from a particular depth from a sample of specified density with unique orientation and proximity to environmental objects. This calculated value is then compared with results of the TL measurements (Appendix 4-11).

In like manner, the measured doses may be back-calculated to provide estimates of free-field kerma independent of sample environment. The consistency of measurement of samples from different locations and laboratories can be made. The disadvantage of this method is that errors associated exclusively with the calculation become incorporated into the transformed TL values.

A more straightforward way to compare consistency of results from the various TL laboratories is to measure identical samples taken from the same location. This comparison was made for tiles from the floor of the roof of Hiroshima University and from bricks taken from the Ieno-cho wall in Nagasaki. The results are listed in Tables 4 and 5 and a dose depth profile of the Ieno-cho brick is shown in Figure 26.

These tests give an indication of the level of agreement obtained between laboratories for the measurement of similar tiles, but they do not address the question of accuracy of the measurements.

Accuracy of measurement was examined in a specifically designed blind study. Extracted, annealed Nagasaki brick crystals were irradiated at NBS with a $^{60}Co$ gamma-ray dose that was unknown to the measuring laboratories (Appendix 4-10). Unfortunately only two of the laboratories had completed the analysis prior to disclosure of the applied doses, so the study was not blind to all of the laboratories making the measurements. These measurements were made with the techniques used by the various laboratories for the analysis of other samples

## Table 5. Intercomparison: Nagasaki Ieno-cho Wall, Dose/depth.

| Lab. | Sample | Sample I.D. # | Section | Depth (mm) | TL Method* | Gross (Gy)†† Unadjusted | Gross (Gy)†† Adjusted** | Laboratory Averages Lab. | Gross (Gy)†† Unadjusted | Gross (Gy)†† Adjusted** |
|---|---|---|---|---|---|---|---|---|---|---|
| Dur | Ieno wall | NAIEO5 | A | 03-32 | PD MA,MAD | 1.10 | 1.20 | Dur (A) | 1.03 | 1.12 |
| Dur | Ieno wall | NAIEO5 | A | 03-32 | HT | 0.95 | 1.04 | | | |
| J.N.I.R.S | Ieno wall | A | A | 10-30† | PD | 1.20 | 1.20 | J.N.I.R.S. (A) | 1.20 | 1.20 |
| J.N.I.R.S | Ieno wall | B | A | 5-20 | PD | 1.21 | 1.21 | | | |
| N.U.E. | Ieno wall | A | A | 02-36 | HT | 1.14 | 1.12 | N.U.E. (A) | 1.14 | 1.12 |
| Oxf H | Ieno wall | NAIEO5 | A | 03-32 | HT | 0.95 | 1.01 | OxfH (A) | 0.95 | 1.01 |
| U. of U. | Ieno wall | NAIE06 | A | 04-36 | PD MA | 0.97 | 1.08 | U. of U. (A) | 0.97 | 1.08 |
| Dur | Ieno wall | NAIEO5 | B | 34-64 | PD MA,MAD | 0.78 | 0.85 | Dur (B) | 0.82 | 0.89 |
| Dur | Ieno wall | NAIEO5 | B | 34-64 | HT | 0.85 | 0.93 | | | |
| J.N.I.R.S | Ieno wall | A | B | 30-70† | PD | 1.02 | 1.02 | J.N.I.R.S. (B) | 1.05 | 1.05 |
| J.N.I.R.S | Ieno wall | B | B | 35-50 | PD | 1.08 | 1.08 | | | |
| N.U.E. | Ieno wall | B | B | 36-70 | HT | 1.03 | 1.01 | N.U.E. (B) | 1.03 | 1.01 |
| Oxf H | Ieno wall | NAIEO5 | B | 34-64 | HT | 0.80 | 0.85 | OxfH (B) | 0.80 | 0.85 |
| U. of U. | Ieno wall | NAIE06 | B | 37-69 | PD MA | 0.79 | 0.88 | U. of U. (B) | 0.79 | 0.88 |
| Dur | Ieno wall | NAIEO5 | C | 66-103 | PD MA,MAD | 0.82 | 0.89 | Dur (C) | 0.76 | 0.83 |
| Dur | Ieno wall | NAIEO5 | C | 66-103 | HT | 0.70 | 0.76 | | | |
| J.N.I.R.S | Ieno wall | A | C | 70-102† | PD | 0.79 | 0.79 | J.N.I.R.S. (C) | 0.86 | 0.86 |
| J.N.I.R.S | Ieno wall | B | C | 65-102† | PD | 0.93 | 0.93 | | | |
| N.U.E. | Ieno wall | C | C | 70-104 | HT | 0.98 | 0.96 | N.U.E. (C) | 0.98 | 0.96 |
| Oxf H | Ieno wall | NAIEO5 | C | 66-103 | HT | 0.73 | 0.77 | OxfH (C) | 0.73 | 0.77 |
| U. of U. | Ieno wall | NAIE06 | C | 70-102 | PD MA | 0.66 | 0.74 | U. of U. (C) | 0.66 | 0.74 |

Unadjusted Values: (Dose to Quartz††)

| Depth | Mean (Gy) | Stdev (Gy) | Stdev (%) |
|---|---|---|---|
| A | 1.06 | 0.11 | 11% |
| B | 0.90 | 0.13 | 14% |
| C | 0.80 | 0.12 | 15% |

NBS adjusted values: (Dose to Quartz††)

| Depth | Mean (Gy) | Stdev (Gy) | Stdev (%) |
|---|---|---|---|
| A | 1.11 | 0.07 | 7% |
| B | 0.90 | 0.09 | 10% |
| C | 0.85 | 0.09 | 10% |

† Two depths combined
†† Dose to quartz inclusive of background

*HT = High Temperature
PD = Pre-dose
MA = Pre-dose Multiple Activation
MAD = Pre-dose Modified Additive Dose

**Correction factors based on intercalibration using NBS irradiated MSO

| | |
|---|---|
| DUR | 1.09 |
| JNIRS | 1.00 |
| NUE | 0.98 |
| OXF | 1.06 |
| U of U | 1.11 |

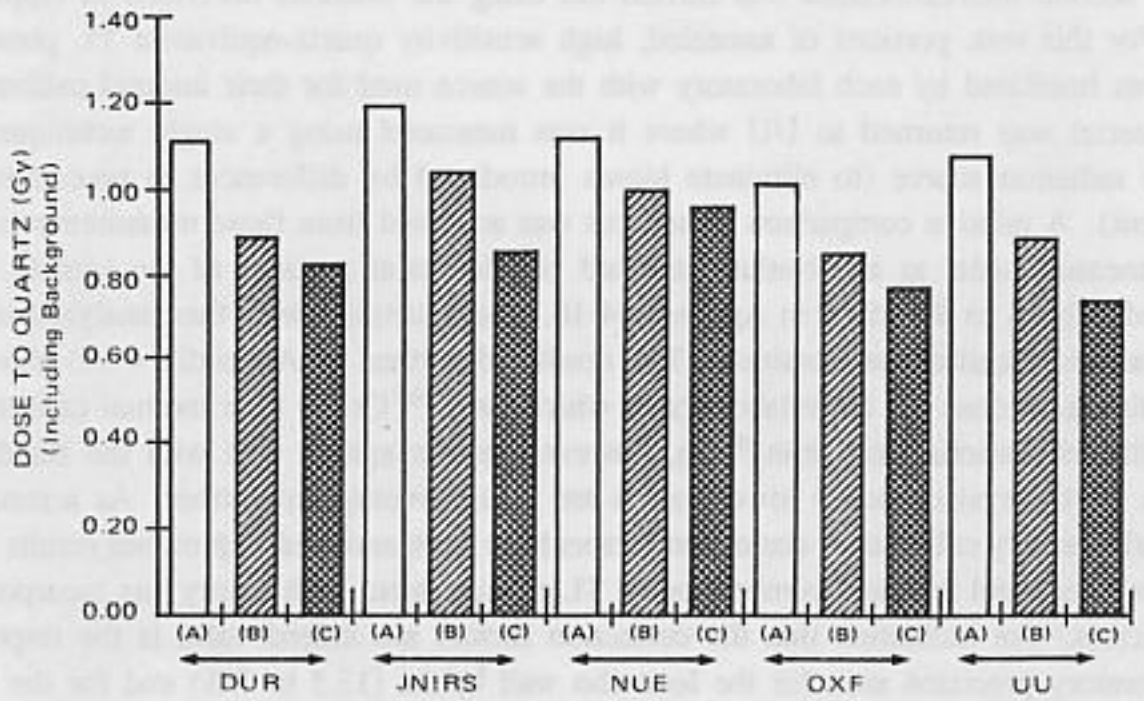


*Figure 26. Ieno-cho dose/depth profile by laboratory.*

Table 6. Percent Error in Measurement of NBS-irradiated Ieno-cho Samples by Laboratory.

| | Sample 1 0.082 Gy | Sample 2 0.163 Gy | Sample 3 0.417 Gy |
|---|---|---|---|
| DUR | - | - | 11.0% |
| JNIRS | −2.4% | 11.0% | 4.1 |
| NUE | −14.6 | 3.7 | −5.8 |
| OXF | - | - | −13.7 |
| UOFU | −12.2 | 0.0 | 16.5 |

Calibration factors included DUR = 1.09; JNIRS = 1.00; NUE = 0.98; OXF = 1.06; UU = 1.11.

from Hiroshima and Nagasaki. The test did not yield sufficient precision, however, to permit the results to be used for determining small differences in source calibration between the laboratories. Results of the analyses are shown in Table 6.

**Intercalibration of Sources**

The accuracy of calibration of the radiation sources used by each laboratory was the subject of two tests. The first was a relative test of source calibration between the laboratories using quartz irradiated at OXF and distributed to the other laboratories. Each laboratory measured the material and reported the measured dose based upon that laboratory's internal calibration. Because of appreciable changes in sensitivity following the first heating, analysis of the sample was not straightforward and a number of different methods were tried at the various laboratories. Large uncertainties were associated with these measurements and a second intercalibration test was required.

The second intercalibration was carried out using the methods described in Appendix 4-10. For this test, portions of annealed, high sensitivity quartz-equivalent TL phosphor MSO was irradiated by each laboratory with the source used for their internal calibration. The material was returned to UU where it was measured using a single technique and a single radiation source (to eliminate biases introduced by differences in procedures or equipment). A relative comparison of sources was achieved from these measurements. To tie the measurements to an absolute standard two identical portions of the sample were irradiated at NBS as described in Appendix 4-10. These samples were then analyzed at UU and an absolute calibration obtained. The results (described in Appendix 4-10) show an underestimate of dose for those laboratories which used $^{137}Cs$ for their internal calibration. Where the irradiations were with $^{60}Co$, however, results agreed well with the standards. Reasons for the systematically lower values are being investigated further. As a result of this interlaboratory calibration, correction factors have been assigned to previous results from each laboratory and the final comparison of TL measurement with theory has incorporated these factors. An indication that the correction factors are indeed valid is the improved interlaboratory precision seen for the Ieno-cho wall bricks (13.3 to 9%) and for the floor tiles from the roof of the Faculty of Sciences building (5.2 to 3.4%) when the calibration factors are included (Tables 4 and 5).

**Relationship to Earlier Results**

A large number of tile samples from buildings which are no longer in existence were analyzed in the 1960s.[1,2] Since the inclusion of the results of analyses of these samples extends the range over which measurements may be compared with theory, it is worthwhile examining them critically for possible sources of error.

Hashizume et al[2] used a technique of sample preparation in which the tile matrix was crushed to a powder and used for TL analysis without further preparation . The sample was heterogeneous and composed of a variety of particle sizes and compositions. The alpha-particle component of dose would have been impossible to determine with this method of preparation; however, the A-bomb doses were sufficiently high that the natural doses from alpha, beta, and gamma radiation were insignificant. Nevertheless the heterogeneous composition of the samples could have resulted in problems with TL properties, particularly since curve matching techniques were used for TL analysis. A recent study sheds light on the validity of the early sample measurements.

A somewhat indirect check of the effect of sample heterogeneity was the work performed by Stoneham (Appendix 4-9) on thin sections of tile from Hiroshima University. These sections, approximately 250 $\mu$m in thickness by 1.2 cm in diameter, were not treated in acid and no attempt was made to obtain a "purified solution". The material was composed of the exact minerals constituting the uncrushed tile; had Hashizume et al[2] measured tiles from Hiroshima University they would have been similar in mineral composition, if not matrix structure, to those of Stoneham. The close agreement that Stoneham reached with other TL techniques performed on the same tiles by laboratories using other contemporary techniques tends to support the early results obtained at JNIRS. Nonetheless, the earlier tiles were not from Hiroshima University and had been crushed to a powder unlike Stoneham's thin sections.

**Agreement of Measurements with Calculated Values**

In Appendix 4-11 Kaul et al detail comparisons of measurement with values calculated for those locations. Two points stand out: (1) measured values are significantly lower than calculated values in Nagasaki, where the principal source of data is from the Ieno-cho bricks, and (2) measured values are significantly higher than calculated values for the tiles collected in Hiroshima at virtually all locations.

Three laboratories (UU, OXF, and DUR) were limited in the number and locations of samples that were available to them for analysis. In Hiroshima, the Faculty of Sciences Building at Hiroshima University was the only building examined by these laboratories and a single location on that building (1449 m from the hypocenter) was the only site analyzed by OXF and DUR. In Nagasaki, the Ieno-cho wall (1428 m from the hypocenter) was the only site measured by the three laboratories.

It is possible to compare the values obtained by the laboratories at these two locations with values derived from theory (Figures 27 and 28); however, the comparison with theory at other locations must rely on the values obtained principally by two laboratories (NUE and JNIRS). At the common measurement location at Hiroshima University (1449 m) the calculated value (50 rad) was lower than the net measured value (69 rad) excluding the JNIRS value (which appears to be an outlier) by an average of 38%. The agreement between the

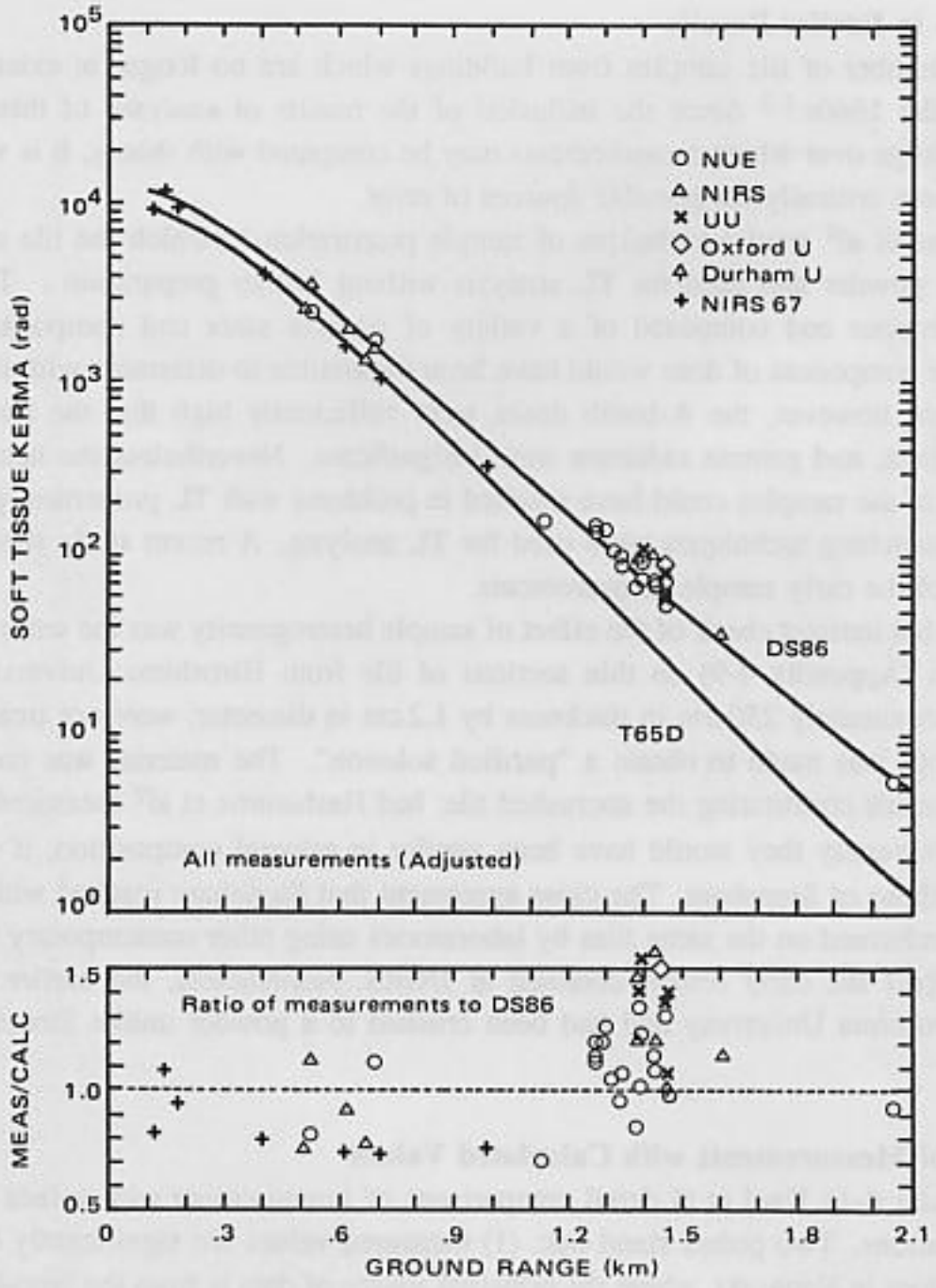


*Figure 27. Comparison of theoretical calculations with measurements. Free-field kerma in soft tissue versus distance from hypocenter at Hiroshima (Appendix 4-11).*

four laboratories on the gross measurements is better than 5% (one sigma). Maximum spread is low, with the gross measurement from OXF differing from NUE measurements by 12%. The agreement of NUE with the OXF, DUR, and UU laboratories is reassuring, since the majority of samples from Hiroshima were analyzed by NUE. The fact that calculations differ significantly from measurements at this location is less reassuring. However, when the values from 21 locations measured by NUE are compared with calculation of dose the agreement improves considerably, resulting in less than 10% difference between measured and calculated values. Nevertheless, measurements by UU at four other nonshielded locations on the Faculty of Science building at Hiroshima University exceed calculated values by 36%, and measurements by JNIRS at six other sites at Hiroshima University exceed calculations

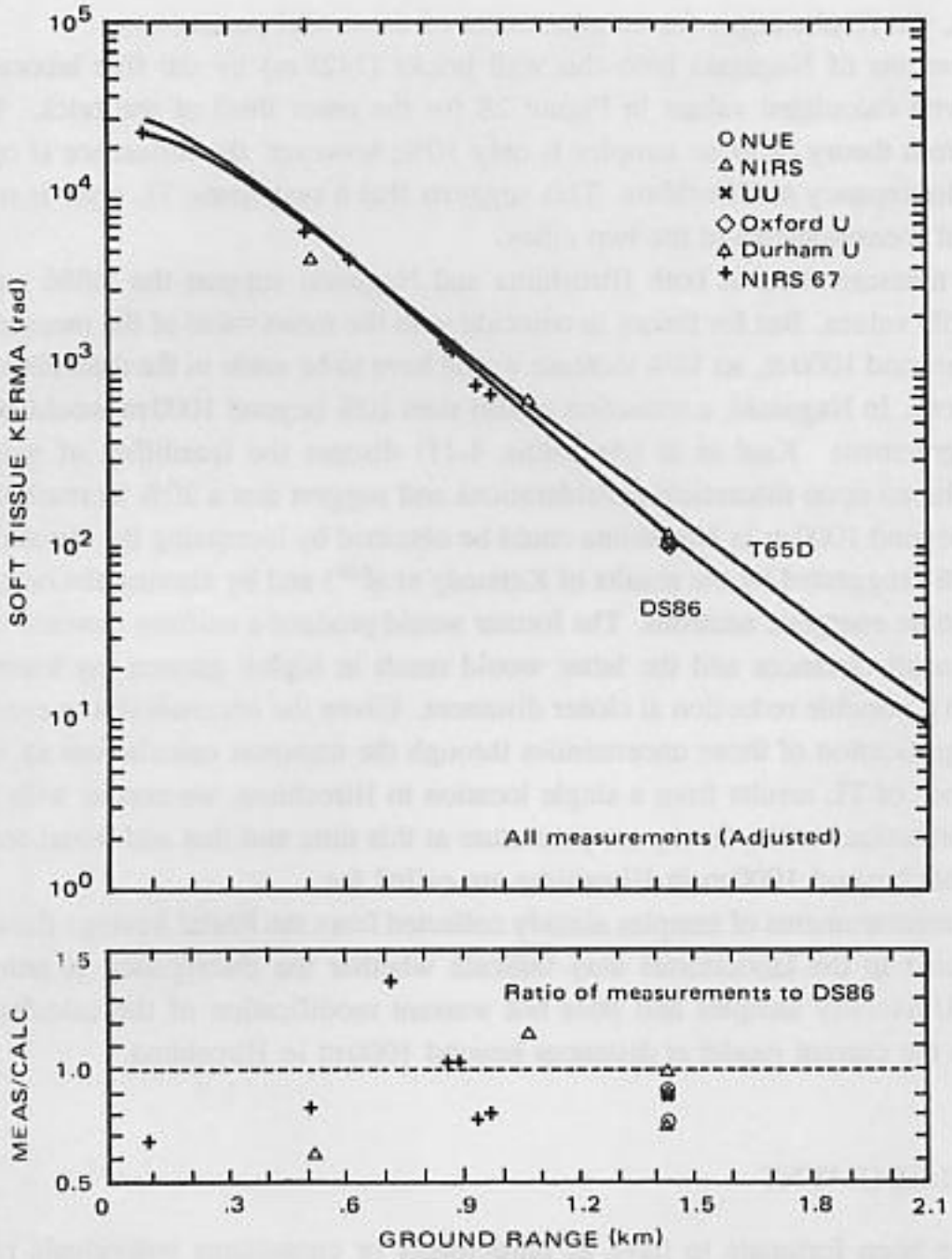


*Figure 28. Comparison of theoretical calculations with measurements. Free-field kerma in soft tissue versus distance from hypocenter at Nagasaki (Appendix 4-11).*

by 28%. Measurements of all of the laboratories differ significantly from calculated values at disances beyond 1000 m in Hiroshima (NUE, $p<0.01$; JNIRS, $p<0.005$; UU and DUR combined, ($p<0.001$).

Figure 27 shows results of measurements compared with theory for all of the Hiroshima locations. The greater value of measured to calculated dose is clearly evident at distances greater than 1000 m for all of the laboratories; 24 of 28 measurements exceed calculated values. The reverse appears to be true at distances less than 1000 m with 10 of 14 measurements being lower than the calculated values. However, agreement improves at this distance if only contemporary measurements are included.

Since the area beyond 1000 m is the region of greatest importance in terms of number

of survivors, the results argue for an adjustment of the model parameters.

Measurements of Nagasaki Ieno-cho wall bricks (1428 m) by the five laboratories are compared with calculated values in Figure 28 for the outer third of the brick. The mean difference from theory of these samples is only 10%; however, the difference is opposite to that of the discrepancy at Hiroshima. This suggests that a systematic TL error is not biasing the results of measurements at the two cities.

Current measurements at both Hiroshima and Nagasaki support the DS86 calculations over the T65D values. But for theory to coincide with the mean value of the measurements in Hiroshima beyond 1000 m, an 18% increase would have to be made in the theoretical model at these distances. In Nagasaki, a reduction of less than 10% beyond 1000 m would be required for exact agreement. Kaul et al (Appendix 4-11) discuss the feasibility of making such corrections based upon theoretical considerations and suggest that a 20% increase in gamma-ray kerma beyond 1000 m in Hiroshima could be obtained by increasing the Hiroshima bomb yield by 10% (suggested by the results of Kennedy et al[29]) and by altering the output spectra to produce more energetic neutrons. The former would produce a uniform increase in gamma-ray kerma at all distances and the latter would result in higher gamma-ray kerma beyond 1000 m with a possible reduction at closer distances. Given the uncertainties in cross sections and the magnification of those uncertainties through the transport calculations as well as the preponderance of TL results from a single location in Hiroshima, we concur with Kaul et al that such corrections to the theory are premature at this time and that additional comparative measurements beyond 1000 m in Hiroshima are called for.

Further measurements of samples already collected from the Postal Savings Bank (1600 m) and distributed to the laboratories may indicate whether the discrepancy is unique to the Hiroshima University samples and does not warrant modification of the calculations or is universal to the current model at distances beyond 1000 m in Hiroshima.

## ACKNOWLEDGMENT

We have been fortunate to have as participants or consultants individuals responsible for development of the current techniques. The Research Laboratory for Archaeology and the History of Art under the guidance of Professor Martin Aitken has been responsible for development of many of the TL techniques which address the needs of this study. We are also grateful to Dr. Stewart Fleming and Dr. Stephen Sutton for their many insights and contributions, and to Ian Bailiff, Doreen Stoneham, and John Huxtable for their work on this project.

## REFERENCES

1. Ichikawa Y., Higashimura T., Shidei T., 1966. Thermoluminescence dosimetry of gamma rays from atomic bombs in Hiroshima and Nagasaki. Health Physics 12:395-405.
2. Hashizume T., Maruyama T., Shiragai A., Tanaka E., Izawa M., Kawamura S. and Nagaoka S., 1967. Estimation of the air dose from the atomic bombs in Hiroshima and Nagasaki. Health Physics 13:149-161..

3. Daniels, F., 1967. Early studies of thermoluminescence radiation dosimetry. In *Luminescence Dosimetry*, Proceedings of the International Conference on Luminescence Dosimetry, Stanford University, 1965, pp. 34-43. Washington: Department of Energy report CONF-650637.

4. Grogler, N., Houtermans, F.G., and Stauffer, H., 1960. Ueber die Datierung von Karamik und Ziegel durch Thermolumineszenz. Helvetica Physica Acta 33:595-596.

5. Kennedy, G.C., and Knopff, L., 1960. Dating by thermoluminescence. Archaeology 13:147-148.

6. McKeever, S.W.S., 1984. Thermoluminescence in quartz and silica. Radiation Protection Dosimetry 8:81-98.

7. McKeever, S.W.S., 1985. *Thermoluminescence of Solids*. Cambridge: Cambridge University Press, solid state science series.

8. Haskell, E.H., Kaipa P.L. and Wrenn M.E., 1984. The use of thermoluminescence analysis for atomic bomb dosimetry: Estimating and minimizing total error In *Second U.S.-Japan Joint Workshop for Reassessment of Atomic Bomb Radiation Dosimetry in Hiroshima and Nagasaki*, pp. 32-44. Hiroshima: Radiation Effects Research Foundation.

9. Fleming, S.J., 1979. *Thermoluminescence Techniques in Archaeology*. Oxford: Clarendon Press.

10. Aitken, M.J., 1974. *Physics and Archaeology*. Oxford: Clarendon Press.

11. Aitken, M.J., 1985. *Thermoluminescence Dating*. London: Academic Press.

12. Fleming, S.J., 1970. Thermoluminescence dating: refinement of the quartz inclusion method. Archaeometry 12:133-147.

13. Fleming, S.J., 1973. The pre-dose technique: a new thermoluminescence dating method. Archaeometry 12:133-147.

14. Zimmerman, D. W., 1971. Thermoluminsecent dating using fine grains from pottery. Archeometry 13:29-52.

15. Huxtable J., and Aitken, M.J., 1985. Conventional TL characteristics of four ornamental tiles from Hiroshima. *Hiroshima/Nagasaki Dose Reassessment Thermoluminescence Workshop*, p.58. Salt Lake City: University of Utah, Radiobiology Division, report COO-119-260.

16. Fleming, S. J., 1975. Supralinearity corrections in fine grain thermoluminescence dating: a reappraisal. Archaeometry 17:122-129.

17. Bowman, S.G.E., 1975. Dependence of supralinearity on pre-dose: some observations. Archaeometry 17:129-132.

18. Bailiff, I.K. and Aitken, M.J., 1980. Use of thermoluminescence dosimetry for evaluation of internal beta dose-rate in archaeological dating. Nuclear Instruments and Methods 173:423-429.

19. Bailiff, I.K., 1983. Pre-dose dating: sensitization of R traps? PACT J. 9:208-214.

20. Bailiff, I.K., 1985. Pre-dose and inclusion dating: An attempted comparison using iron age pottery from Northern Britain. Nuclear Tracks 10:771-777.

21. Thompson, J., 1970. *The Influence of Previous Radiation on Thermoluminescent Sensitivity*. Oxford University: D. Phil. thesis, Faculty of Physical Sciences.

22. Aitken, M.J. and Murray A.S., 1976. The pre-dose technique: radiation quenching. In *The Edinburgh Symposium on Archaeometry and Archaeological Prospection, Extended Abstracts*. London: HMSO.

23. Aitken M.J., 1978. Pre-dose dating: predictions from the model. PACT 3:319-324.

24. Haskell E.H. and Bailiff I.K., 1985. Diagnostic and corrective procedures for pre-dose TL analysis. Nuclear Tracks 10:503-508.

25. Chen, R., 1979. Saturation of sensitization of the 110°C TL peak in quartz and its potential application in the pre-dose technique. PACT 2:325-335.

26. Maruyama, T. Kumamoto, Y., and Noda, Y., 1985. Thermoluminescence dosimetric techniques and their application to evaluation of A-bomb dose in Hiroshima and Nagasaki. *Hiroshima/ Nagasaki Dose Reassessment Thermoluminescence Workshop*, pp. 3-18. Salt Lake City: Univer-

sity of Utah, Radiobiology Division, report COO-119-260.

27. Kaipa P.L. and Haskell E.H., 1985. In situ dosimetry of intact ceramic using the sensitized 210 °C TL peak of quartz. Nuclear Tracks 10:621-623.

28. Ichikawa, Y. and Nagatomo, T., 1978. Thermoluminescence dating of burnt sandstones from Senpukuji cave. PACT 2:174-178.

29. Kennedy, L.W., Roth, L.A., and Needham, C.E., 1984. *Calculations to Assist in a New Hiroshima Yield Estimate*. Albuquerque, NM: S-Cubed, report 84-6629/R1.